ISMRM JPC2025

THE 10TH ANNUAL SCIENTIFIC MEETING OF THE ISMRM JAPANESE CHAPTER

DATE

AUGUST 30 (SAT.) ,2025

VENUE

RCREA HIMEJI 2F SMALL HALL

CHAIR

SHIGERU KIRYU, M.D.,Ph.D.
(Department of Radiology, International University of Health and Welfare)

ISMRM Japanese Chapter

大会会長ご挨拶

Welcome from the Meeting Chair

Dear colleagues,

I am honored and pleased to introduce the 10th ISMRM-Japanese Chapter Annual Scientific Meeting.

The International Society for Magnetic Resonance in Medicine (ISMRM) is the world's largest research organization for MRI, with researchers from all over the world participating. The ISMRM-Japan Chapter (ISMRM-JPC) was established in 2016 as the Japanese organization of ISMRM and has been holding annual meetings in Japan. This year's conference is co-hosted with the Japanese Society of Magnetic Resonance in Medicine (JSMRM) and marks its 10th anniversary.

The modalities related to radiology are multidisciplinary, particularly MRI, which has a strong tendency in this regard, involving researchers from diverse fields such as engineering, pharmacy, medicine, computer science, and others. Cutting-edge technologies like artificial intelligence are integrated into this exciting modality from the early stages. The ISMRM-JPC comprises researchers from basic science to clinical applications and share the latest information on MRI. We are also working to enhance Japan's presence within ISMRM.

This year, the event will be held at Arcrea HIMEJI on August 30th. We expect active discussions with many participants and especially hope for the enthusiastic participation of young researchers.

Shigeru Kiryu,M.D.,Ph.D.
Professor and chairman
Department of Radiology, International University of Health and Welfare

第１０回国際磁気共鳴医学会・日本支部学術集会

（The 10th Annual Scientific Meeting of the ISMRM Japanese Chapter）

主　　催

国際磁気共鳴医学会（ISMRM）日本支部

Organized by ISMRM Japanese Chapter

会　　期

2025 年 8 月 30 日（土）30（Sat.）August 2025

会　　場

アクリエひめじ（Arcrea HIMEJI）

〒670-0836 兵庫県姫路市神屋町 143-2

143-2, Kamiyacho, Himeji-city, Hyogo,670-0836

大　会　長

桐生　茂

（国際医療福祉大学 医学部 放射線医学）

Chairs：Shigeru Kiryu,M.D.,Ph.D.

（Department of Radiology, International University of Health and Welfare）

Society Information for the Japanese Chapter of ISMRM

Executive Committee:

Chair:
Shigeru Kiryu, M.D., Ph.D.
International University of Health and Welfare
Chiba, Japan

Vice Chair:
Yuhei Takado, M.D., Ph.D.
National Institutes for Quantum Science and Technology Chiba, Japan

Past Chair:
Masaki Fukunaga, Ph.D.
National Institute for Physiological Sciences
Okazaki, Japan

Secretary General:
Shintaro Ichikawa, M.D., Ph.D.
University of Yamanashi
Yamanashi, Japan

Treasurer:
Masaaki Hori, M.D., D.M.Sc.
Toho University Omori Medical Center
Tokyo, Japan

Membership Secretary:
Shigeru Kiryu, M.D., Ph.D.
International University of Health and Welfare
Chiba, Japan

Advisor:
Seiji Ogawa, Ph.D.
Tohoku Fukushi University
Sendai, Japan

Other Committees:

Program Committee:
Chair: Yoshiyuki Watanabe, M.D., Ph.D.
Financial Strategy Committee:
Chair: Yoshiharu Ohno, M.D. Ph.D.
Election Administrating Committee:
Chair: Kazuhiro Nakamura, Ph.D.
Inspectors:
Masafumi Harada, M.D., Ph.D.
Yoshichika Yoshioka, Ph.D.
Society Relations Committee:
Chair: Koji Sakai, Ph.D.
Industry-Academy Relations Committee:
Chair: Hiroyuki Kabasawa, Ph.D.
Code Improvement Committee:
Chair: Ichio Aoki, Ph.D.

Financial Committee:
Chair: Masaaki Hori, M.D., D.M.Sc.
Public Relations Committee:
Chair: Yuichiro Matsuoka, Ph.D.
Nominating Committee:
Chair: Yasuo Takehara, M.D., D.M.Sc.
Awards Committee:
Chair: Yoshiharu Ohno, M.D. Ph.D.

Future Planning Committee:
Chair: Hiroaki Terasawa, Ph.D.
Young Investigators Committee:
Chair: Sosuke Yoshinaga, Ph.D.

第１０回　国際磁気共鳴医学会・日本支部学術集会　査読者

The 10th Annual Scientific Meeting of the ISMRM Japanese Chapter Reviewer List

青木 伊知男（Ichio Aoki）先生

市川 新太郎（Shintaro Ichikawa）先生

桐生　茂（Shigeru Kiryu）先生

高堂 裕平（Yuhei Takado）先生

竹原 康雄（Yasuo Takehara）先生

堀　正明（Masaaki Hori）先生

福永 雅喜（Masaki Fukunaga）先生

松岡 雄一郎（Yuichiro Matshuoka）先生

渡邉 嘉之（Yoshiyuki Watanabe）先生

（五十音順／Japanese order）

本年は査読者の投票による奨励賞を設けましたので表彰します。

座長・演者へのご案内

座長へのご案内

・プログラムの円滑な進行のため、各セッションの時間管理をお願いいたします。

・英語セッションをご担当いただく座長の先生方は、発表者が英語で聴衆へ説明する際や討議を行う場合に、発表者をサポートいただけますようお願いいたします。

・本大会では、す演者の略歴を準備しておりません。現所属のアナウンスのみでお願いいたします。

・座長受付はございません。

・ご担当セッション開始予定時刻の 15 分前までに、会場内右手前方の進行席のスタッフへお声掛けいただき、「次座長席」にご着席ください。

演者へのご案内

■利益相反（COI）に関する情報開示について

・本大会では、利益相反の開示が必要となります。

・スライドの最初（または演題・発表者などを紹介するスライドの次）に、利益相反（COI）状態を開示してください。

※詳細は、以下をご参照ください。

https://www.c-linkage.co.jp/jsmrm2025/abstracts.html

■発表データ

・Microsoft PowerPoint で作成・編集してください。

・発表スライドは、ワイドサイズ（16：9）で作成をお願いいたします。

・ご発表データのファイル名は、「演題番号」と「氏名」をご入力ください。

■PC 受付

1）発表データの受付

ご発表の 30 分前までに必ず第 53 回日本磁気共鳴医学会大会のＰＣ受付で発表データの試写をお願いいたします。

2）PC 受付での発表データの修正作業は準備進行の妨げになりますのでご遠慮ください。

3）事前にご自身でウイルスチェックを必ず行ってください。

4）Macintosh での発表データを作成される場合は、ご自身の PC 本体をお持込みください。

5）動画及び音声をご使用の場合は、ご自身の PC 本体をお持込みください。

6）お預かりした発表データは、終了後に PC より消去いたします。

■PC 本体をお持込みの方

1）PC 本体をお持込みの方は、PC 受付でデータ確認終了後、発表会場の PC オペレーター席（会場内手前方）まで、ご自身で PC 本体をお持ちください。

2）PC 本体をお持込みの場合は、外部ディスプレイ出力が可能であることを、必ずご確認ください。

3）会場内には、PC プロジェクターにつながった HDMI ケーブル、及び D-Sub15 ピン（ミニ）オスを用意しております。

※Mini Display Port など上記以外のコネクターについては、変換コネクターの貸出を行っておりませんので、必ずご持参ください。

4）PC の AC アダプターは、必ず各自でご持参ください。

一般演題（口述発表）演者の方へ

・口述発表の発表時間は、12 分（発表 7 分、質疑 5 分）です。

・演者受付はございません。

・セッション開始予定時刻の 15 分前までに、会場内左手前方の「次演者席」にご着席ください。

円滑な進行のため、時間厳守でお願いいたします。

会場（Venue）

アクリエひめじ（Arcrea HIMEJI）　2F small hall

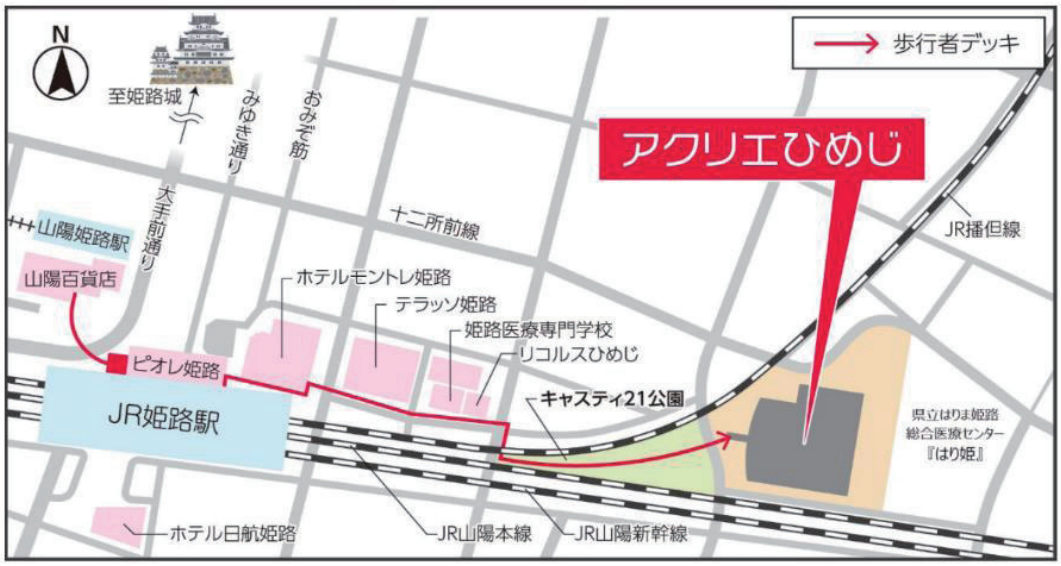

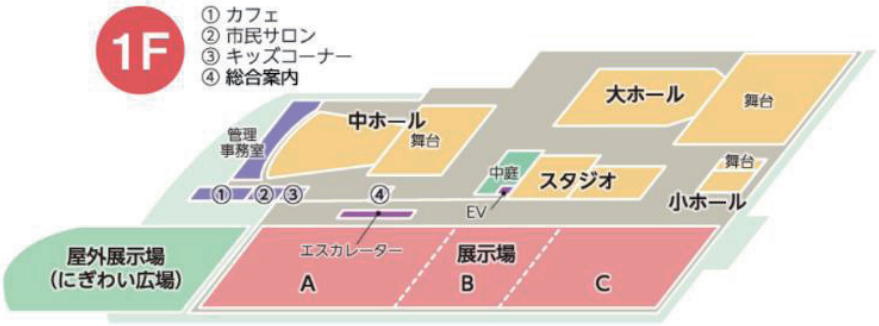

Program

9：45　Opening Remarks

Shigeru Kiryu　(International University of Health and Welfare)

9：50～11：00　Oral Presentation 1

Chair：**Yuhei Takado**　(National Institutes for Quantum Science and Technology)

Speakers

JPC-001　The relationship between brain activity and emotion recognition in social anxiety disorder
Junbing He
(Research Center for Child Mental Development, Chiba University)

JPC-002　The effect of sleep quality on resting-state functional connectivity
Yasuka Sahara
(National Institutes for Quantum Science and Technology)

JPC-003　Impact of respiratory and cardiac physiological noise correction on EPI quantitative susceptibility mapping time series
R. Allen Waggoner
(RIKEN Center for Brain Science)

JPC-004　UV-Induced Hyperpolarization for In Vivo 13C-MRI in Awake Mice: A Comparison with Trityl Radical Method
Maiko Ono
(Institute for Quantum Life Science, National Institute for Quantum Science and Technology)

JPC-005　Oxygen-enhanced MRI of the brain using 3D VIBE and 3D MR fingerprinting
Yasutaka Fushimi
(Department of Diagnostic Imaging and Nuclear Medicine, Graduate School of Medicine, Kyoto University)

JPC-006　Cerebral Edema in the Global Ischemia: Intrathecal H 2 17 O-MRI in a Cardiac Arrest Model
Takaaki Fujii
(Department of Diagnostic Imaging, Graduate School of Medicine, Hokkaido University)

11：10～12：20　Oral Presentation 2

Chair： **Yoshiyuki Watanabe**　(Shiga University of Medical Science)

Speakers

JPC-007　Comparison of 3D Diagonal and 3-Scan Trace Diffusion-Weighted Imaging for Breast MRI
Yusuke Jo
(Department of Radiology, Anjo Kosei Hospital)

JPC-008　Automated Breast Cancer Detection and Classification Using Machine Learning on DWI
Kaito Nonoyama
(Department of Radiology, Nagoya University Graduate School of Medicine)

JPC-009　Usefulness of real-time sequence management in abdominal DWI MRI
Yuji Ohizumi
(Department of Radiology, International University of Health and Welfare Narita Hospital)

JPC-010　Exploring Structural Brain Differences in OCD and SAD Using VBM and SBM
Nadire Aximu
(Department of Cognitive Behavioral Physiology, Graduate School of Medicine, Chiba University)

JPC-011　Cognitive traits and brain functions in older adults during the stroop task
Kazuya Ouchi
(University of Tsukuba)

JPC-012　Hemostatic Radiotherapy for Gastric Cancer: MRI as an Alternative to Endoscopy for Post-Treatment Evaluation
Osamu Tanaka
(Department of Radiation Oncology, Asahi University)

13：40～14：00　Work in Progress

Chair：**Shintaro Ichikawa**　(University of Yamanashi)

Speakers

AIRS Medical Japan
SwiftMR™: A Software-Based, Vendor-Neutral DLR AI for Instantly Improved MRI Image Quality and Reduced Scan Time

Sunghwan Lee
(AIRS Medical Japan G.K.)

United Imaging Healthcare Japan
Innovations in MRI: Recent Advances from UIH
Kathy Kong
(Shanghai United Imaging Healthcare co., ltd)

14：10～15：10　Symposium 1　ISMRM hot topics

Chair：**Ichio Aoki**　(National Institutes for Quantum Science and Technology)

Speakers

Program Chair Report of ISMRM Hawai'i Meeting
Kei Yamada
(Department of Radiology, Kyoto Prefectural University of Medicine)

Small Animal Imaging and Clinical Breast MRI: Lessons from ISMRM 2025
Mami Iima
(Department of Fundamental Development for Advanced Low Invasive Diagnostic Imaging, Nagoya University Graduate School of Medicine)

Latest Topics from ISMRM 2025: Focusing on AI reconstruction
Yasuhiko Terada
(University of Tsukuba)

15：20～16：20　Symposium 2　AI, Radiomics

Chair：**Shigeru Kiryu**　(International University of Health and Welfare)

Speakers

The Evolution and Frontiers of Radiomics:Exploring the Future of Medical AI through Image-Derived Data
Koji Sakai
(Clinical AI Research Lab., Department of Radiology, Kyoto Prefectural University of Medicine)

Artificial intelligence in radiology: from CNN to LLM
Koichiro Yasaka
(Department of Radiology, The University of Tokyo Hospital)

The Foundations, Rapid Advancements, and Medical Applications of AI—And What Comes Next
Hitoshi Iyatomi
(Department of Applied Informatics, Faculty of Science and Engineering, Hosei University)

16：30～16：50　Ogawa Seiji Prize Lecture

Chair：**Masafumi Harada**　(Tokushima University)

Speakers

2-Nitroimidazole-Functionalized Superparamagnetic Iron Oxide Nanoparticles Detect Hypoxic Regions of Glioblastomas on MRI and Improve Radiotherapy Efficacy
Yuki Yoshino
(Department of Radiology, Kyoto Prefectural University of Medicine)

17：00～17：30　Oral Presentation 3

Chair：**Yuichiro Matsuoka**　(Gunma Paz University)

Speakers

JPC-013　MR Elastography for Brain Tumors: Initial Experience
Tatsuya Oki
(Department of Radiology, Shiga University of Medical Science)

JPC-014　Clinical Feasibility: MR Elastography-based Slip Interface Imaging for Assessment of Myofascial Interface Mobility in Chronic Low Back Pain
Emi Hojo
(Mayo Clinic, Rochester, Minnesota)

JPC-015　Evaluation of skeletal muscle energy metabolism before and after exercise using CEST MRI
Chisato Ando
(Department of Radiological Technology, Graduate School of Health Science, Juntendo University)

Symposium ISMRM hot topics

Program Chair Report of ISMRM Hawai'i Meeting

Kei Yamada
Department of Radiology,Kyoto Prefectural University of Medicine

It was an incredible privilege to serve as Program Chair for the 2025 ISMRM Meeting. The theme for Honolulu was "ISMRM: Towards a healthier footprint." We built a few sessions related to this theme, including Ernst Plenary.

There were a few new initiatives for this meeting and I would like to describe some of those below.

Lowering the Language Barrier

As an international society, reducing communication stress among attendees is beneficial. We planned the following three initiatives at the beginning of my term, among which we executed the first one (extra moderators) this year. The rest will be kept in our wish-list and will undergo further discussion in the following years.

1. Extra Moderators: This year we added a third multilingual moderator to assist presenters during the Q&A sessions. We asked the presenters whether they would want someone who speaks their own language, and there were 103 respondents who wished to have this support. Thus, the demand is high, and we plan to continue this in future years.
2. Automatic Translation Using Artificial Intelligence (AI): We planned to place a sub-screen for presenters and attendees displaying AI-translated English text. This tool would help presenters understand questions during the Q&A sessions. Owing mainly to the cost, we decided to postpone this for the future years.
3. Pre-recording: We planned to allow video presentations for those who experience stage fright or those with speech disorders (i.e. stuttering). This will help alleviate the anxiety of presenters with language barriers. Since this initiative could lead to facilitation of no-shows, there were discussions about how we should notify the members about this initiative. This year, we offered chance to record their presentations when we noticed that the presenters were hesitant to give talks in Oral Sessions.

Registered Studies

This is a new initiative by the Reproducibility Study Group. This category enables presenters to submit pre-registered studies. They had about half a year to complete their experiments, which were submitted in April as digital posters. Acceptance rate of these abstracts was not high as many of them did not meet the criteria of registered studies.

Reducing the Size of Contents While Elevating Quality

Our motivation for compressing the meeting contents comes primarily from the survey results, which indicated that there is too much to see/experience during the week. There were also opinions about the lack of enough time for networking. Therefore, we tried to make this meeting slightly more compact by implementing the following measures: Eliminating the Thursday Sunrise Sessions (7:00-8:00) , Eliminating the "We are One" Session on Thursday Morning, Shortening the ceremony for YIA on Thursday, Reducing the Size of the Clinical Focus Meeting (CFM), Eliminating the "Shark-tank" Session, Eliminating the Fireside Chats.

Plenary Sessions

The named lectures were given by 3 outstanding scientists:

- Reza Razavi, UK, Cardiac imaging (Mansfield, Sunday)

Symposium ISMRM hot topics

- Shintaro Ichikawa, ROW, Liver imaging (NIBIB, Tuesday).
- Kim Butts-Pauly, US, Neuromodulation (Lauterbur, Thursday)

We offered 4 Plenary Sessions entitled:

- From bits to qubits: Advancing medical diagnosis with quantum-powered AI (Monday)
- Crosstalk in liver-cardio-brain function (Tuesday)
- Sustainability in industry (Ernst plenary) (Wednesday)
- Open-source revolution: reproducible sequences, hardware and reconstruction algorithms (Thursday)

I am hoping that the program this year was enjoyable. As a final comment, I would like to convey my special gratitude towards the members of AMPC, especially the table chairs. I am also grateful to the past AMPC chairs, particularly Brian Hargreaves for taking time to guide me through the whole process. Finally, I thank the next program chairs Katy Keenan and Stephan Maier as well as the Central Office Staff, for their endless patience and experience.

Figure
Photograph of AMPC members taken during the construction meeting at Sheraton Lisboa Hotel & Spa, January 2025.

Symposium ISMRM hot topics

Curriculum Vitae

Kei Yamada

Dr. Yamada received his medical degree from Kyoto Prefectural University of Medicine (KPUM). After his residency training, he moved to the USA for fellowship training at several institutions, including University of Maryland, University of Rochester, and Harvard Medical School (Massachusetts General Hospital). During his stay in Rochester, he received Winthrop fellow of the year (1996). He came back to Japan and became a junior faculty member of the KPUM in 1999. He was subsequently promoted to the position of Professor and Chair of Radiology in 2012. He was asked to take key roles in various organizations, including serving as a President of JCR, Secretary General of AOSNHNR, and Program Chair of ISMRM (Honolulu 2025).

Symposium ISMRM hot topics

Small Animal Imaging and Clinical Breast MRI: Lessons from ISMRM 2025

Mami Iima, MD, PhD

Department of Fundamental Development for Advanced Low Invasive Diagnostic Imaging,

Nagoya University Graduate School of Medicine,Nagoya, Japan

Abstract

This presentation explores how small animal MRI research contributes to advancing clinical imaging techniques, with insights from recent ISMRM presentations.

Small animal models provide an essential platform for developing and validating innovative MRI methods in controlled environments. Through these preclinical studies, researchers can explore novel contrast mechanisms, optimize imaging protocols, and understand fundamental biological processes before clinical translation. Recent advances demonstrate successful translation of metabolic imaging, molecular targeting approaches, and advanced diffusion techniques from animal models to clinical applications.

The presentation will highlight examples of how preclinical findings have improved tumor detection, characterization, and treatment monitoring. These translational successes underscore the importance of maintaining strong connections between basic research and clinical practice.

Symposium ISMRM hot topics

Curriculum Vitae

Mami Iima

Mami lima is a radiologist and Designated Professor of the Department of Fundamental Development for Advanced Low Invasive Diagnostic Imaging, Nagoya University Graduate School of Medicine. Following her clinical training at Kyoto University Faculty of Medicine, she studied in France at NeuroSpin, an ultra-high field MRI research center, where she obtained her Ph.D. degree. After working at Kyoto University's Hakubi Center and the university hospital's Diagnostic Imaging and Nuclear Medicine Department, she assumed her current position in 2023. Her main research interest is to establish innovative diagnostic imaging methods for breast cancer using both clinical trials and preclinical models by means of various modalities, including diffusion MRI. She has published more than 80 papers, among them valuable articles about IVIM and diffusion MRI in the breast in addition to a comprehensive IVIM review. Mami Iima has received several important awards for her contribution to the field of IVIM and diffusion MRI in oncology.

Symposium ISMRM hot topics

Latest Topics from ISMRM 2025: Focusing on AI reconstruction

Yasuhiko Terada

Institute of Pure and Applied Sciences, University of Tsukuba

Technological advances in MRI, as demonstrated at ISMRM 2025, are primarily driven by AI. There has been a shift from theoretical research to practical clinical applications. In this presentation, I will focus on AI-based reconstruction and review the five major trends characterizing this transition, highlighting key sessions. First, I will present how AI addresses the clinical challenge of "motion and noise," as demonstrated in O-08, "AI-Based Real-Time Imaging & Motion-Robust Strategies." Next, I will outline approaches such as self-supervised learning to address the issue of "data scarcity," as discussed in O-09, "Riding the Frontier of MRI Reconstruction." Third, I will cover key themes from D-06, "Quantitative imaging," regarding the transition to quantitative imaging diagnosis. Fourth, I will review the ultra-high-speed examination technologies presented in the "AI-Based Acquisition & Reconstruction" poster series (beginning with D-22), which aim to improve clinical efficiency. Lastly, I will show the importance of "clinical application and validation" and explore the path to practical utility. This is based on the content discussed in sessions such as “O-14: “AI: Image Analysis & Software" and "O-16: AI-Enhanced Imaging: Redefining Clarity & Precision.” This review presents a comprehensive report on the maturity and future prospects of AI in MRI based on the content presented at the ISMRM 2025 conference.

Curriculum Vitae

Yasuhiko Terada

BUSINESS ADDRESS
Institute of Pure and Applied Sciences,
University of Tsukuba, Tsukuba, 305-8573 Japan.
E-mail: terada.yasuhiko.fu@u.tsukuba.ac.jp

EDUCATION

1992.4-1994.3 The University of Tokyo, College of Arts and Science
1994.4-1996.3 The University of Tokyo, Department of Applied Physics, Faculty of Engineering,
Bachelor of Engineering
1996.4-1998.3 The University of Tokyo, Department of Applied Physics, Graduate School of Engineering, Master of Engineering
1998.4-2001.3 The University of Tokyo, Department of Applied Physics, Graduate School of Engineering, Doctor of Engineering

EMPLOYMENT RECORD

2001.4-2004.3	Postdoctoral Researcher, Advanced Research Laboratory, Hitachi Co. Ltd.
2004.4-2005.3	Postdoctoral Researcher, National Institute for Materials Science
2005.4-2008.5	Postdoctoral Researcher, University of Tsukuba
2008.6-2016.1	Assistant Professor, University of Tsukuba
2016.2-Present	Associate Professor, University of Tsukuba

RESEARCH INTEREST

Development of novel MRI systems, New applications in MRI

ACADEMIC AND OTHER PROFESSIONAL ACTIVITIES

2010.6-Present	Member of Japanese Society for Magnetic Resonance in Medicine
2011.5-Present	Member of International Society for Magnetic Resonance in Medicine

Symposium AI, Radiomics

The Evolution and Frontiers of Radiomics: Exploring the Future of Medical AI through Image-Derived Data

Koji Sakai
Clinical AI Research Lab., Department of Radiology, Kyoto Prefectural University of Medicine

Overview: Radiomics is an emerging analytical approach that extracts and quantifies a large number of features from medical images to characterize diseases beyond what is visible to the naked eye. In this lecture, I will outline the historical development of Radiomics and highlight cutting-edge clinical applications, particularly in combination with artificial intelligence (AI), offering insights into the future of data-driven diagnostics.

1. Foundations and Historical Development

First proposed by Aerts et al. in 2012 [1], Radiomics aims to move beyond qualitative interpretation by providing a quantitative analysis of imaging data. Initially applied in oncology, features such as texture, shape, and intensity were extracted from CT and MRI to support prognosis prediction and therapy response assessment. Since then, the field has expanded with advancements in 3D feature extraction, standardized preprocessing protocols (e.g., IBSI guidelines), and improved feature selection methods, enhancing reproducibility and technical reliability [2].

2. Recent Trends and Clinical Applications

Current radiomics research is expanding beyond oncology into a wide range of fields, including neurodegenerative diseases, inflammatory conditions, and cardiovascular diseases. Since 2020, major topics have included the integration of genomics and electronic health record data ("multi-omics radiomics") [3], studies related to COVID-19 pneumonia [4], integrated analysis with AI [5], multi-modality and multi-center research [6], the application of deep radiomics (deep feature extraction) [7], and the integration of explainable AI (XAI) [8].

3. Challenges and Future Directions

Despite its potential, Radiomics still faces several challenges for clinical translation, including issues of standardization, reproducibility, and interpretability of algorithms. Future developments are expected to focus on the integration with explainable AI (XAI) systems to ensure both high prediction performance and clinical trustworthiness. This lecture aims to provide researchers and clinicians with a practical understanding of how Radiomics can be leveraged in real-world medical contexts.

References: **[1]** Aerts HJWL, et al. *Nat Commun.* 5:4006 (2014) **[2]** Zwanenburg A, et al. *Radiology.* 295(2):328-338 (2020) **[3]** Kang W, et al. *J Transl Med* 21:598 (2023). **[4]** Homayounieh F, et. al. *Radiology.* 2(4): (2020) **[5]** Zhang YP, et. al. *Military Med Res.* 10:22 (2023). **[6]** Xiong L, et al. *Breast Cancer Research.* 26:157 (2024) **[7]** Saadh MJ, et al. BMC *Musculoskelet Disord.* 26:498 (2025). **[8]** Haupt M, et al. *Diagnostics.* 15(11):1399 (2025)

Symposium AI, Radiomics

Curriculum Vitae

Koji Sakai

Current Affiliation
Clinical AI Research Laboratory Department of Radiology
Graduate School of Medical Science

Kyoto Prefectural University of Medicine

EDUCATION
1987 – 1991 Bachelor of Engineering (Applied Chemistry),
Iwate University (Japan)
1992 – 1994 Mater of Engineering (Applied Chemistry),

Iwate University (Japan)

2001 – 2004 PhD. Software and Information Science,

Iwate Prefectural University

Working History

1991 - 1994 Researcher, Seiko Chemical Co. Ltd. (Japan)
1994 - 2000 Researcher, Iwate Institute Research Center (Japan)
2000 - 2004 Researcher, Research Institute for Environmental Sciences and Public Health of Iwate Prefecture (Japan)

Academic Appointments

2004 - 2009 Assistant Professor Center for Promotion of the Excellence in Higher Education Kyoto University (Japan)
2007 - 2008 Visiting Researcher Department of Radiology, Graduate school of Medicine, Johns Hopkins University (USA)
2009 – 2011 Assistant Professor Department of Human Health Science, Graduate school of Medicine, Kyoto University (Japan)
2015 - 2017 Associate Professor Advanced MR Imaging Research Laboratory, Department of Radiology Graduate School of Medical Science, Kyoto Prefectural University of Medicine (Japan)

Symposium AI, Radiomics

2018 – current Associate Professor Clinical AI Research Laboratory, Department of Radiology
Graduate School of Medical Science, Kyoto Prefectural University of Medicine (Japan)

Professional Affiliations and Scientific Publications

Professional Affiliations:
Delegate member of JSMRM 2024
Committee member of JSMRM (Communication, Editor, International) 2018 –
Board member of JSMI (Future planning) 2023 -
Chair of JSMI (Communication) 2025 –
Chair of ISMRM-JPC (Society relation committee) 2025-
Selected Publications:

Books

1. Imaging of Neurodegenerative Disorder, Sangam G. Kanekar Ed., Part IV. Alzheimer's disease, Chapter 10. Mild Cognitive Impairment, pp. 90-112, Thieme Medical Publishers, Inc., ISBN 978-1-60406-854-2, 2015
2. Clinical MRI At Your Fingertips, Taro Takahara Ed.,II4 Diffusion tensor image and evolution, pp. 285-288, Medical View Co., Ltd, ISBN 978-4-7583-0894-6 C3047, 2013
3. MR Buzzology, H H Schild, (Japanese) Yokio Miki, Shinichi Urayama, Koji Sakai, Tetsuya Yoneda, 2013
4. Magnetic Resonance Imaging Clinics：Advances in diffusion-weighted imaging, Temperature Measurement by Diffusion-Weighted Imaging, p253-261. Elsevier (2021)

Papers

1. Koji Sakai, et al., Age-dependent brain temperature decline as assessed by DWI thermometry, *NMR in Biomedicine*, 2011; 24(9): 1063–1067
2. Koji Sakai, et al., Calculation methods for ventricular DWI thermometry: phantom and volunteer studies, *NMR in Biomedicine*, 2012; 25(2), 340-346
3. Koji Sakai, et al., Can we shorten the q-space imaging to make it clinically feasible?, *Japanese Journal of Radiology*, 2017; 35: 16-24.
4. Koji Sakai, et al., Does cerebrospinal fluid pulsation affect DWI thermometry? A study in healthy volunteers, *NMR in Biomedicine,* ; 35(8): e4738

Symposium AI, Radiomics

Atificial intelligence in radiology: from CNN to LLM

Koichiro Yasaka

Department of Radiology, The University of Tokyo Hospital

We are currently in the midst of the artificial intelligence (AI) boom. Large language models (LLMs) have gained widespread social acceptance. This boom was triggered by the advent of AlexNet, a type of convolutional neural network (CNN) that achieved remarkable performance compared to conventional models in an image recognition competition held in 2012. Since the mid-2010s, deep learning applications have gained increasing attention in the field of radiology. Along with advances in deep learning technologies, their applications in radiology have become more diverse, including lesion detection, image processing, and natural language processing. In this talk, we review the applications of deep learning technologies in radiology.

Symposium AI, Radiomics

Curriculum Vitae

Koichiro Yasaka

Work history

2024 – present Specially appointed lecturer, Department of Radiology, The University of Tokyo Hospital, Japan

2021 - 2024 Assistant Professor, Department of Radiology, The University of Tokyo Hospital, Japan

2016 - 2021 Assistant Professor, Department of Radiology, IMSUT Hospital, The Institute of Medical Science, The University of Tokyo, Japan

Education

2012 - 2016 Ph.D. Graduate School of Medicine, The University of Tokyo, Japan

2002 - 2008 M.D. Faculty of Medicine, The University of Tokyo, Japan

International Awards

1. 2024 RSNA Honored Educator Award (RSNA, 2024)
2. "Radiology" Editor's Recognition Award with Distinction (RSNA, 2025)
3. "Radiology" Editor's Recognition Award with Special Distinction (RSNA, 2024)
4. "Radiology" Editor's Recognition Award with Distinction (RSNA, 2023)
5. "Radiology" Editor's Recognition Award with Special Distinction (RSNA, 2022)
6. "Radiology" Editor's Recognition Award with Distinction (RSNA, 2021)
7. "Radiology" Editor's Recognition Award with Special Distinction (RSNA, 2020)

Representative Publications as a First Author

1. A New Step Forward in the Extraction of Appropriate Radiology Reports. Radiology 2025;315:e250867
2. Fine-Tuned Large Language Model for Extracting Patients on Pretreatment for Lung Cancer from a Picture Archiving and Communication System Based on Radiological Reports. J Imaging Inform Med 2025;38:327
3. Super-resolution Deep Learning Reconstruction for 3D Brain MR Imaging: Improvement of Cranial Nerve Depiction and Interobserver Agreement in Evaluations of Neurovascular Conflict. Acad Radiol 2024;31:5118
4. Deep learning reconstruction for 1.5 T cervical spine MRI: effect on interobserver agreement in the evaluation of degenerative changes. Eur Radiol 2022;32:6118
5. Deep learning and artificial intelligence in radiology: Current applications and future directions. PLoS Medicine 2018;15:e100270
6. Liver fibrosis: Deep convolutional neural network for staging by using gadoxetic acid-enhanced hepatobiliary phase MR Images. Radiology 2018;287:146
7. Deep learning with convolutional neural network for differentiation of liver masses at dynamic contrast-enhanced CT: A preliminary study. Radiology 2018;286:887

Symposium AI, Radiomics

The Foundations, Rapid Advancements, and Medical Applications of AI—And What Comes Next

Hitoshi Iyatomi
Department of Applied Informatics, Faculty of Science and Engineering, Hosei University

In recent years, AI technologies—exemplified by OpenAI's ChatGPT and Google's Gemini, have undergone remarkable advancements. These models now possess not only the ability to understand and generate text, but also multi-modal generative capabilities such as producing images, music, and program code. As a result, they are exerting a profound and accelerating impact on our society and everyday lives. In this lecture, I will provide a broad overview of AI technologies from foundational principles to practical applications and future perspectives, structured around the following four themes:

1. Fundamental principles of intelligent processing in AI

To begin, I will reflect on how computers, once regarded merely as fast calculators, have come to perform intelligent tasks. I will briefly explain the fundamental concept of "learning" that lies at the core of AI, and introduce the "attention mechanism," a pivotal technology that underpins the advanced intelligent processing seen in modern AI systems.

2. What is "Generative" AI? – Differences from traditional AI and its Potential

Next, I will explore the nature of generative AI, which has seen especially rapid development in recent years. I will clarify what "generation" entails and highlight how it differs conceptually from previous AI approaches. Additionally, I will provide an overview of multi-modal AI that can process text and images in an integrated manner.

3. Applications of Generative AI in the medical field

The core of this talk will focus on recent research efforts that apply cutting-edge generative AI technologies to medicine. I will showcase recent achievements and trends, particularly in tasks such as diagnostic support and the detection of regions of interest, including organs and pathological findings.

4. AI Agents: Future prospects and big concerns of Next-Generation AI

Finally, I will introduce the concept and potential of AI agents, which are expected to become increasingly prevalent in the near future. AI agents are next-generation systems that not only leverage the reasoning capabilities of AI models, but also autonomously interact with their environment by utilizing external APIs and databases to accomplish complex, general-purpose tasks. I will outline their fundamental architecture and use cases, while also discussing the societal and ethical concerns that arise alongside the hope they bring, drawing on real-world examples.

Symposium AI, Radiomics

Curriculum Vitae

Hitoshi Iyatomi

Dr. Hitoshi Iyatomi, Ph.D in Engineering,
Ph.D in Medical Science.Professor,
Department of Applied Informatics,
Hosei University Faculty of Science and Engineering.
E-mail: iyatomi@hosei.ac.jp
Webpage: http://iyatomi-lab/front-e.html

Professional experience: (Current positions are indicated in bold)

2004 - present Hosei University
2024/4- Dean of the Graduate School of Science and Engineering
2023/4- Chief of the Department of Applied Informatics, Graduate School of Science and Engineering
2018/4-2020/3 Chair of the Department of Applied Informatics, Faculty of Science and Engineering
2018/4- Professor, Department of Applied Informatics Faculty of Science and Engineering
2014/4-2016/3 Head of Student Affairs Office at Koganei Campus
2011/4-2018/3 Associate Professor,
2008/4-2011/3 Lecturer, Department of Applied Informatics Faculty of Science and Engineering.
2004/4-2008/3 Research Associate,
Department of Electrical Informatics, Faculty of Engineering.
2016/4-2017/3 Visiting Scholar, Johns Hopkins University
2007/4- present Visiting Lecturer, Department of Dermatology, Tokyo Women's Medical University.
2004/6 -2017/3 Visiting Researcher, Department of Dermatology, Keio University School of Medicine
2000/4-2004/3 Technical Consultant, Hewlett-Packard Japan Co. Ltd.

Education:

2011/12 Ph.D in Medical Science, Graduate School of Medicine, Tokyo Women's Medical University.
2004/3 Ph.D in Engineering, Graduate School of Keio University, School of Science and Technology.
2000/3 M.E. in Electrical Engineering, Graduate School of Keio University, School of Science and Technology.
1998/3 B.E in Department of Electronics, Keio University Department of Science and Technology.

Publications

Dr. Iyatomi has authored or co-authored over 170 peer-reviewed journals and conference papers across various machine learning-based research areas, including computer vision, medical engineering, natural language processing, and more.
Google Scholar: https://scholar.google.com/citations?user=ghyQxvIAAAAJ
Researchmap: https://researchmap.jp/read0165542

Ogawa Seiji Prize Lecture

2-Nitroimidazole-Functionalized Superparamagnetic Iron Oxide Nanoparticles Detect Hypoxic Regions of Glioblastomas on MRI and Improve Radiotherapy Efficacy

Yuki Yoshino
Department of Radiology, Kyoto Prefectural University of Medicine
Department of Radiation Oncology, Osaka Medical and Pharmaceutical University

The presence of hypoxic regions in tumors is associated with malignancy and is an important target for high-precision diagnosis and treatment of tumors. Radioresistant hypoxic regions can be precisely identified and treated without the use of high doses of radiation if hypoxic region-specific contrast agents have a therapeutic effect. In this study, we synthesized a therapeutic-diagnostic complex agent (SPION-PG-NI) by combining polyglycerol-functionalized superparamagnetic iron oxide nanoparticles (SPION-PG, core diameter 8.8 ± 1.9 nm) as an MRI contrast agent and 2-nitroimidazole (NI, a pimonidazole derivative) as a hypoxia-targeted ligand to visually evaluate hypoxic regions using MRI and improve radiotherapy efficacy at those sites. SPION-PG-NI showed a concentration-dependent contrast effect and had significantly higher accumulation in subcutaneous glioblastomas than the control agent, SPION-PG, 24 h after administration. Immunohistological evaluations showed that the SPION-PG-NI-accumulated regions corresponded well with hypoxic regions. SPION-PG-NI showed neither migration into the brain parenchyma nor neurotoxicity. Both SPION-PG and SPION-PG-NI decrease reactive oxygen species (ROS); however, they improve radiotherapy efficacy in hypoxic glioblastoma cells due to cytotoxicity. This effect of SPION-PG-NI was significantly higher than SPION-PG ($p < 0.01$). After 12 Gy irradiation, the mean normalized glioblastoma tumor volume on 38 d in the SPION-PG-NI group (288%) was significantly lower than that in the control group (882%) ($p < 0.05$). Collectively, these findings suggest the potential of SPION-PG-NI as a useful and safe tumor theranostic nanodevice for hypoxic imaging and improving radiotherapy efficacy.

Ogawa Seiji Prize Lecture

Curriculum Vitae

Yuki Yoshino

Yuki Yoshino (Doctor of philosophy
(doctor of medicine.) and Master of science)

Affiliation：cross-appointment contract

1. Department of Radiology, Kyoto Prefectural University of Medicine, Assistant professor.
2. Department of Radiation Oncology, Osaka Medical and Pharmaceutical University, Assistant professor.

E-mail: yyoshino@koto.kpu-m.ac.jp　　yuki.yoshino@ompu.ac.jp

Academic background

Year	
2004	Graduate from Department of Science, Kyoto University
2006	Master's degree in Radiation Biology, Graduate School of Science, Kyoto University
2014	Graduate from the School of Medicine, Kyoto Prefectural University of Medicine
2024	Ph.D. in Medical Science, Kyoto Prefectural University of Medicine

License

2014	Licensed Medical Doctor	Japan
2021	Certified Radiation Oncologist	The Japan Radiological Society (JRS)・ Japanese Society for Radiation Oncology (JASTRO)
2022	Certified Training Supervisor in Radiation Oncology	JRS
2024	Certified Physician for Boron Neutron Capture Therapy (BNCT)	Japanese Society of Neutron Capture Therapy (JSNCT)

Personal Statement

Engaged in both clinical practice and research in the field of radiation oncology at Kyoto Prefectural University of Medicine and Osaka Medical and Pharmaceutical University. At Kyoto Prefectural University of Medicine, while providing clinical care, I am actively working to translate research findings on MRI-based imaging of tumor hypoxia into clinical applications. At Osaka Medical and Pharmaceutical University, I am primarily involved in the clinical practice and research of boron neutron capture therapy (BNCT), with ongoing efforts to evaluate the distribution of novel boron agents in tumors and throughout the body using MRI.

Work in Progress

Work in Progress

SwiftMR™: A Software-Based, Vendor-Neutral DLR AI for Instantly Improved MRI Image Quality and Reduced Scan Time

Sunghwan Lee
Managing Director, AIRS Medical Japan G.K.

Magnetic Resonance Imaging (MRI) is an essential diagnostic modality. Yet, the persistent trade-off between image quality and scan time continues to limit diagnostic clarity, timely access to care, and patient throughput. SwiftMR, developed by AIRS Medical, is a vendor-neutral, deep learning-based software that directly addresses this longstanding challenge—enabling both image enhancement and scan time reduction simultaneously.

SwiftMR employs a Deep Learning Reconstruction (DLR) model trained on paired DICOM datasets: fully sampled images alongside under-sampled counterparts that have been synthetically degraded across multiple raw-data dimensions affecting noise and resolution. This architecture enables robust denoising and super-resolution enhancement directly from DICOM inputs—without requiring hardware upgrades or vendor-specific sequences. As a result, SwiftMR can reduce scan time by up to 50%, regardless of scanner vendor and model, magnetic field strength, imaging sequence, or anatomy. It is effective even in challenging settings such as older systems, low-field systems, pediatric exams, or 3D imaging sequences like angiography.

Now deployed in over 550 medical institutions across 30 countries—including numerous leading university and general hospitals—SwiftMR has shown measurable real-world benefits: improved patient satisfaction, enhanced interpretability, reduced patient backlog, and harmonization of image quality across heterogeneous MRI systems.

This presentation will introduce the core technology behind SwiftMR, discuss integration into clinical workflows, highlight representative use cases, and share validation results from peer-reviewed research. SwiftMR provides a scalable and cost-effective pathway to enhance diagnostic performance, patient experience, and MRI productivity—without the capital investment or operational disruption typically required for hardware upgrades.

Work in Progress

Work in Progress

Innovations in MRI: Recent Advances from UIH

Kathy Kong. Ph.D.
MR Product Manager,Shanghai United Imaging Healthcare co., ltd

United Imaging Healthcare (UIH) is committed to advancing medical imaging through the development of core technologies and global deployment of imaging systems.
The uMR Jupiter 5T, equipped with a 5T superconducting magnet and high-performance RF system, is being developed as an ultra-high-field MRI system with potential applications in both clinical and research settings.
Meanwhile, the uMR Ultra integrates high-density RF, powerful gradient performance, and AI-driven technologies via the uAIFI.LIVE platform, aiming to enable dynamic and flexible imaging capabilities.
Both systems are designed to support use in clinical practice as well as research, and ongoing collaborations and technical validations are helping to explore their utility across various environments.

Oral Presentation 1

JPC-001

The relationship between brain activity and emotion recognition in social anxiety disorder

Junbing He[1,2], Nadire Aximu[1,3], Eiji Shimizu[1,2,3], Yoshiyuki Hirano[1,2]

[1]Research Center for Child Mental Development, Chiba University, [2]United Graduate School of Child Development, Osaka University, [3]Department of Cognitive Behavioral Physiology, Chiba University

Introduction: Social anxiety disorder (SAD) is a prevalent psychiatric disorder. Several studies have found neurocognitive dysfunction in SAD patients[1,2]. However, few studies have discussed the relationship between cognitive dysfunction and brain activity in SAD patients. Therefore, the aim of this study was to explore the abnormal brain activity of SAD patients and to investigate the relationship between abnormal brain activity and cognitive function.

Materials & Methods: rs-fMRI data were collected from 27 SAD patients and 40 healthy controls (HCs). Differences in the fractional amplitude of low frequency fluctuation (fALFF) between the two groups were examined to identify regions showing abnormal brain activity. The Cambridge Neuropsychological Test Automated Battery (CANTAB) was used to evaluate cognitive function related to facial emotion recognition (Figure1). Correlations between fALFF and cognitive function were analyzed.

Results: Compared with HCs, SAD patients showed lower mean fALFF (mfALFF) in the bilateral postcentral gyrus (Figure2). The mfALFF was not significantly correlated with any of the clinical symptoms; however, it was significantly correlated with the function of emotion recognition (Figure3).

Discussion: The postcentral gyrus, which belongs to the primary somatosensory cortex area, is a key region responsible for somatosensory processing. In this study, the result suggests that both SAD patients and HCs rely on the postcentral gyrus for perceiving emotion-related information, and that the postcentral gyrus is more closely associated with a surprised face, as observed in previous studies[3].

Conclusions: Abnormal fALFF values in the postcentral gyrus may play an important role in the neural mechanisms of SAD, particularly in sensorimotor processing and emotion recognition.

References:

1. Okawa, S., Hamatani, S., Hayashi, Y., Arai, H., Nihei, M., Yoshida, T., Takahashi, J., Shimizu, E., & Hirano, Y. (2020). Neuropsychological Comparison Between Patients with Social Anxiety and Healthy Controls: Weak Central Coherence and Visual Scanning Deficit. *Neuropsychiatric Disease and Treatment*, *16*, 2849–2855. https://doi.org/10.2147/NDT.S283950

2. O'Toole, M. S., & Pedersen, A. D. (2011). A systematic review of neuropsychological performance in social anxiety disorder. *Nordic Journal of Psychiatry*, *65*(3), 147–161. https://doi.org/10.3109/08039488.2011.565801

3. Zhao, K., Zhao, J., Zhang, M., Cui, Q., & Fu, X. (2017). Neural Responses to Rapid Facial Expressions of Fear and Surprise. *Frontiers in Psychology*, *8*, 761. https://doi.org/10.3389/fpsyg.2017.00761

Figures

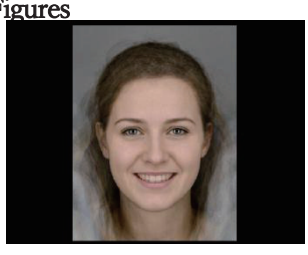

Figure1. Test screen of the Emotional Recognition Task (ERT) originated from the CANTAB.

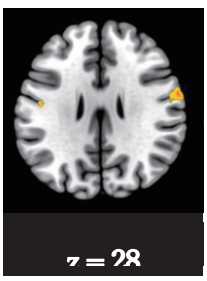

Figure2. Lower mfALFF in bilateral postcentral gyrus in SAD patients compared to HCs.

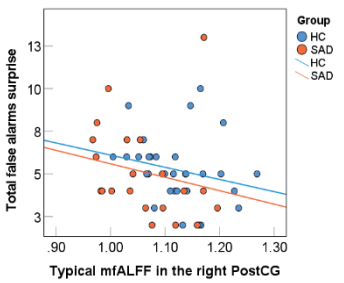

Figure3. Correlations between mfALFF and facial emotion recognition (especially, surprise).

Oral Presentation 1

JPC-002

The effect of sleep quality on resting-state functional connectivity

Yasuka Sahara[1,2], Makiko Yamada[1], Yoshiyuki Hirano[1,3,4], Daisuke Matsuyoshi[1], Haruki Nishimura[1,5], Yasunori Aizawa[1,6], Noriaki Yahata[1], Eiji Shimizu[2,3,4], Takayuki Obata[1,3,4]

1: National Institutes for Quantum Science and Technology, 2: Graduate School of Medicine, Chiba University, 3: Research Center for Child Mental Development, Chiba University, 4: United Graduate School of Child Development, 5: The Ohara Memorial Institute for Science and Labour, 6: Tohoku University Graduate School of Medicine

Introduction: Although many studies have suggested that abnormal sleep may affect resting functional connectivity[1,2], the impact of normal everyday sleep quality on connectivity has been largely ignored. This study investigates the impact of natural sleep quality on the subsequent day's resting-state functional MRI (rsfMRI) connectivity patterns.

Materials & Methods: Fourteen healthy female subjects participated in two sets of tests that included sleep assessments and MRI scans across two consecutive days. Sleep quality was objectively measured using a portable EEG monitor in the participant's home environment. The ROI-to-ROI connectivity was calculated with the CONN toolbox. Multi-regression analysis was used to investigate the relationship between the ROI-to-ROI connectivity and the objective sleep indices. The relationship between the sleep indices and the connectivities was analyzed using repeated measures correlation analysis.

Results and Discussion: Changes to the wake after sleep onset (WASO) and spindle duration (SpD) indexes were correlated with changes in the connectivity between the default mode network (DMN) and salience network (SN). An increase in the SpD index was found to be related to an increase in the connectivity within the SN (Fig.1). Subjects that had large changes in connectivity tended to have substantial changes in WASO between the two measurements. In contrast, even though there may have been a substantial change in connectivity for a particular subject, the accompanying change in SpD was relatively small (Fig.2).

Conclusions: The results suggest that the WASO index is related to the DMN-SN interconnectivity, with the observed alteration in connectivity potentially arising from day-to-day variations in the index. In contrast, changes in connectivity associated with the SpD index may reflect differences between individuals rather than daily fluctuations.

References: [1] Tagliazucchi E, Laufs H., Decoding wakefulness levels from typical fMRI resting-state data reveals reliable drifts between wakefulness and sleep, Neuron., 2014 [2] Lunsford9Avery JR et al., Sleep/Wake Regularity Associated with Default Mode Network Structure among Healthy Adolescents and Young Adults, Sci Rep., 2020

Fig 1.

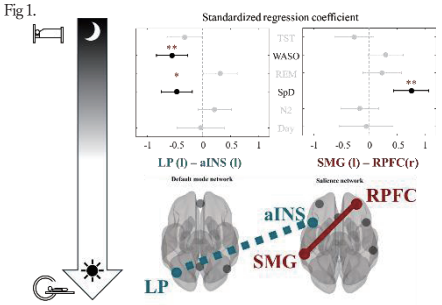

Figure 1. Standardized regression coefficients and independent sleep index (** < .001, * < .005). Sleep assessment and MRI scanning were conducted on 2 consecutive days.

Fig 2.

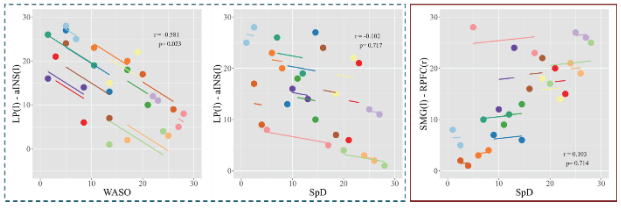

Figure 2. Repeated measures correlations between the sleep indices and connectives. Abbreviations: TST, Total Sleep Time; WASO, Wake After Sleep Onset; REM, Rapid Eye Movement; SpD, Spindle duration; N2, Stage N2.

Oral Presentation 1

JPC-003

Impact of respiratory and cardiac physiological noise correction on EPI quantitative susceptibility mapping time series

R. Allen Waggoner[1], Oliver C. Kiersnowski[2], Kenichi Ueno[1], Luca Roccatagliata[2,3], Chisato Suzuki[1], Mauro Costagli[2,3]

[1]RIKEN Center for Brain Science, Wako-shi, Japan
[2]IRCCS Ospedale Policlinico San Martino, Genova, Italy
[3]University of Genova, Genova, Italy

Introduction The impact of physiological noise is known to affect the echo planar imaging (EPI) phase of the complex MRI signal, more than the magnitude[1,2], however, the effect of physiological noise correction (PNC) on EPI phase and its associated effects on the Quantitative Susceptibility Mapping (QSM) processing pipeline[3] has not been thoroughly investigated. We, therefore, investigated the effects of respiratory and cardiac PNC on EPI phase and outputs of each step of the QSM pipeline.

Methods Multi-echo 2D-EPI[4] magnitude and phase data were acquired on a Siemens Prisma 3T MRI system. Four healthy volunteers were presented with flickering checkerboard stimuli with a stimulus duration of 0.5 s over three consecutive runs. TE = 14.4, 35.3, 56.1, 77.0 ms; TR = 1.6 s; 2 mm isotropic resolution; MB = 4; R = 3; PF = 7/8.

For PNC, pulse oximetry and respiratory data were acquired simultaneously with the EPI acquisitions using a BioPac MP150 system. PNC was applied using an in-house RETROICOR[5] program on the real and imaginary components of the complex-valued images, followed by QSM processing (phase unwrapping with SEGUE[6], background field removal with 2D+3D V-SHARP[7] and susceptibility calculation with iLSQR[8]).

To assess PNC, relative variance (σ_r^2) maps were calculated by evaluating the temporal variance (σ^2) at each TE for each step of the QSM pipeline both before and after PNC was applied. The relative variance is then given by $\sigma_r^2 = \sigma_{afterPNC}^2/\sigma_{beforePNC}^2$ in the range [0, 1].

Results & Discussion Figures show relative variance maps for a representative subject. For each figure the top row shows maps where both respiratory and cardiac PNC have been applied. The middle row shows maps with respiratory PNC applied. The bottom row shows maps with only cardiac PNC applied. Figure 1 shows the dramatic impact of respiratory PNC on the raw phase data. After background field removal, the impact of respiratory and cardiac PNC becomes more similar, with local regions of pronounced noise (Figure 2). Figure 3 highlights a major reduction in relative variance in the brainstem, indicating the large impact of PNC (especially cardiac PNC) in QSM in this region.

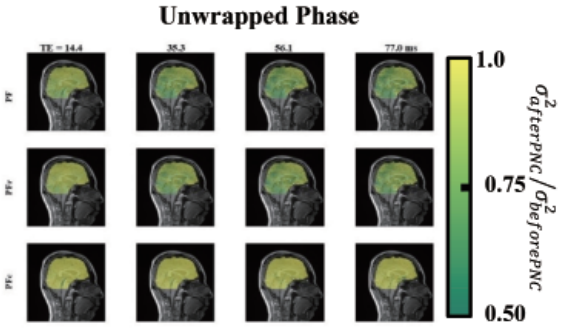

Figure 1. Phase relative variance maps with PNC applied to the real and imaginary components of the image data. PF – both respiratory and cardiac PNC applied to the data. PFr - respiratory PNC applied to the data. PFc - cardiac PNC applied to the data.

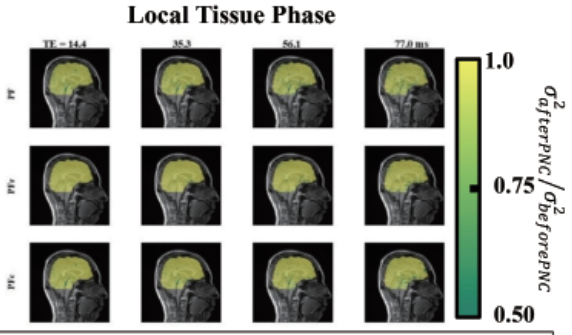

Figure 2. Phase relative variance maps after background field was removed from the PNC corrected phase data. PF – both respiratory and cardiac PNC applied to the data. PFr - respiratory PNC applied to the data. PFc - cardiac PNC applied to the data.

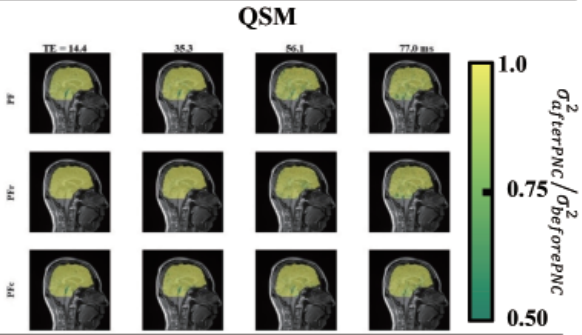

Figure 3. Phase relative variance maps for PNC applied to QSM data. PF – both respiratory and cardiac PNC applied to the data. PFr - respiratory PNC applied to the data. PFc - cardiac PNC applied to the data.

Acknowledgements

This work was partially funded by an Invitational Fellowship from the Japan Society for the Promotion of Science.

References

1. Petridou et al. *Magn Reson Imaging*. 2009;27(8):1046-1057. **2.** Hagberg et al.. *Neuroimage*. 2012;59(4):3748-3761. **3.**QSM Concesus Organization Committee et al. *Magn. Reson. Med.* 2024;91:1834-1862. **4.** https://www.cmrr.umn.edu/multiband/. **5.** Glover et al. *Magn. Reson. Med.* 2000;44:162-167. **6.** Karsa & Shmueli.. *IEEE Trans Med Imaging*. 2019;38(6):1347-1357. **7.** Wei et al.. *NMR Biomed*. 2017;30(4). **8.** Li et al. *Neuroimage*. 2015;108:111-122.

Oral Presentation 1

JPC-004

UV-Induced Hyperpolarization for In Vivo ^{13}C-MRI in Awake Mice: A Comparison with Trityl Radical Method

Maiko Ono[1], Andrea Capozzi[2], Chikara Yamauchi[1], Keita Saito[1], Mor Mishkovsky[3], Yuhei Takado[1]

[1]Institute for Quantum Life Science, National Institute for Quantum Science and Technology, Japan, [2]Poralize, Denmark, [3]École polytechnique fédérale de Lausanne, Switzerland

Introduction: Hyperpolarized ^{13}C-MRI enables real-time visualization of in vivo metabolism and has progressed toward clinical application since its first demonstration in 2003【1】. However, the requirement for close proximity between the polarizer and the MRI system remains a major limitation, owing to the rapid decay of hyperpolarized signal following dissolution. A novel method using UV-induced, non-persistent radicals has emerged as a promising alternative that enables transportable preparation of hyperpolarized agents without the need for trityl radical removal【2,3】. While the technical feasibility of UV-induced hyperpolarization has been demonstrated, its biological applicability in vivo remains underexplored. This study aimed to evaluate the metabolic performance and reproducibility of UV-polarized [1-^{13}C]pyruvate in mice, compared with the conventional Ox63-based approach.

Materials & Methods: Hyperpolarization of [1-^{13}C]pyruvate was performed using either UV-induced radicals (n = 5) or trityl radical Ox63 (n = 5). Each of the five mice underwent scanning under both polarization conditions on separate days, enabling within-subject comparison. Mice were injected intravenously with 10 µL/g body weight of the hyperpolarized solution while awake. Spectroscopic data were acquired using a 3T Bruker system with single-pulse acquisition. Metabolic ratios including Lactate/Pyruvate, Bicarbonate/Pyruvate, and Bicarbonate/Lactate were quantified. Signal variability was evaluated using coefficients of variation (CV), and group comparisons were analyzed using paired t-tests.

Results: Lactate/Pyruvate, Bicarbonate/Pyruvate, and Bicarbonate/Lactate ratios obtained using UV-polarized [1-^{13}C]pyruvate were 0.466 ± 0.053, 0.174 ± 0.030, and 0.376 ± 0.072, respectively, while those obtained with Ox63-polarized pyruvate were 0.519 ± 0.067, 0.179 ± 0.054, and 0.347 ± 0.102. Paired t-tests showed no statistically significant differences between the groups ($p > 0.2$ for all ratios). However, coefficients of variation were consistently lower with UV polarization, indicating enhanced reproducibility: 11.4% vs. 12.9% for Lactate/Pyruvate, 17.2% vs. 29.9% for Bicarbonate/Pyruvate, and 19.2% vs. 29.3% for Bicarbonate/Lactate. Paired line plots demonstrated uniform within-subject trends favoring the UV method in terms of signal stability.

Discussion: Despite producing slightly lower polarization levels, the UV-induced method demonstrated comparable metabolic ratios and improved reproducibility. The superior stability may reflect the chemical purity of the UV-prepared solution, free from residual radicals or co-polarizing agents. This method more closely mirrors clinical practice, where filtered preparations are standard. Planned test–retest studies will further quantify its repeatability and support translational potential.

Conclusions: UV-induced hyperpolarization provides a biologically feasible and technically advantageous alternative to trityl radical-based methods. Its simplicity, stability, and alignment with clinical protocols position it as a promising tool for preclinical and future clinical ^{13}C metabolic imaging.

References:
1. Ardenkjær-Larsen JH, et al. PNAS, 2003 2. Eichhorn et al. PNAS 2013 3. Capozzi et al. arXiv:2503.18537

Oral Presentation 1

JPC-005

Oxygen-enhanced MRI of the brain using 3D VIBE and 3D MR fingerprinting

Yasutaka Fushimi[1], Sachi Okuchi[1], Akihiko Sakata[1], Takayuki Yamamoto[1], Satoshi Nakajima[1], Yuji Nakamoto[1]

[1] Department of Diagnostic Imaging and Nuclear Medicine, Graduate School of Medicine, Kyoto University.

Introduction:

Currently clearance of interstitial fluid (ISF) from the brain is considered to mainly consist of rapid periarterial component (intramural periarterial drainage, IPAD) and slow perivascular component (glymphatic system). We assume OE-MRI can represent rapid drainage from ISF in the brain. We conducted quantitative evaluation of OE-MRI using 3D MRF with the broad dictionary coverage.

Materials & Methods:

Twenty healthy elderly subjects were enrolled in this prospective study. All subjects underwent two phases of pre- and post-oxygen inhalation a 3D MRF: Pre-1, Pre-2, Post-1, and Post-2 at 3T. Between Pre-2 and Post-1, Dynamic 3D VIBE imaging was performed. 3D VIBE: The first measurement of 3D VIBE ($VIBE_{1st}$) was excluded for the analysis. (i) $VIBE_{Nst}$ images were divided by $VIBE_{2nd}$ images ($VIBE_{Nst}/VIBE_{2nd}$). (ii) Pre-O_2 VIBE (average of $VIBE_{2nd}$: $VIBE_{7th}$) and Post-O_2 VIBE (average of $VIBE_{9th}$: $VIBE_{20th}$) were compared. 3D-MRF: Offline reconstruction was performed to create T1 maps for 3D MRF. Dictionary size of MRF was adjusted to cover water as 0-5000 ms for T1. (iii) Pre- and Post-O_2 T1 relaxation time of each phase and (iv) their relative ratios to Pre-1 (rPre2, rPost-1 and rPost-2) were evaluated. Friedman test and ad-hoc Steel-Dwass test were performed to evaluate T1 maps of each mask.

Results:

(i) Dynamic changes of $VIBE_{Nst}/VIBE_{2nd}$ were shown. Rapid signal increase was observed just after O_2 inhalation. (ii) Slight but significant increase was observed in Post-O_2 VIBE compared with Pre-O_2 VIBE. (iii) T1 relaxation time was different at all VOIs among dynamic phases (P values of GM, WM, Surface, and Ventricle were <0.0001, 0.0008, <0.0001, and 0.0242, respectively). Steel-Dwass test showed Post-1 at GM was lower than Pre-1 and Pre-2. (iv) Relative ratios of T1 relaxation time were also different at all VOIs (P values of T1, GM, WM, Surface, and Ventricle were <0.0001, 0.0008, <0.0001, and 0.0242, respectively). Steel-Dwass test showed multiple differences. Specifically, rPost-1 and rPost-2 were lower than Pre-1 at T1_GM; rPost-1 and rPost-2 were lower than Pre-1 and rPre-2 at T1_Surface.

Discussion and Conclusions:

Rapid signal increase on 3D VIBE and decreased T1 relaxation time on 3D MRF was observed especially surface CSF. This rapid change in signal may be due to the rapid transfer of dissolved oxygen into ISF and its subsequent clearance from ISF into CSF. OE-MRI can reflect rapid clearance by IPAD, which can be validated by T1 relaxation time changes derived from 3D-MRF.

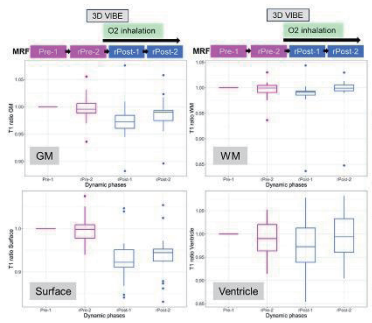

Friedman test	P value
T1_GM	<0.0001
T1_WM	0.0008
T1_Surface	<0.0001
T1_Ventricle	0.0242

Steel-Dwass test		P value
T1_GM	rPost-2 < Pre-1	0.0031
	rPost-1 < rPre-2	0.0032
	rPost-1 < Pre-1	<0.001
T1_WM	rPost-1 < rPost-2	0.0051
	rPost-1 < Pre-1	<0.001
T1_Surface	rPost-1 < rPre-2	0.0002
	rPost-2 < rPre-2	0.0003
	rPost-1 < Pre-1	<0.001
	rPost-2 < Pre-1	<0.001
T1_Ventricle	N/A	

References

1. Nedergaard M. Science 2013;340(6140):1529-1530.
2. Morris AW. Acta Neuropathol 2016;131(5):725-736.
3. Saito S. Front Neurol 2019;10:490.

Oral Presentation 1

JPC-006

Cerebral Edema in the Global Ischemia: Intrathecal $H_2{}^{17}O$-MRI in a Cardiac Arrest Model

Takaaki Fujii[1,2], Hiroyuki Kameda[2,3,4], Yoshitaka Bito[1,3], Naoya Kinota[1,2], Daisuke Kato[1,2], Xiawei Bai[1], Simi Zhou[1], Kohsuke Kudo[1,2,3]

[1] Department of Diagnostic Imaging, Graduate School of Medicine, Hokkaido University, [2] Department of Diagnostic and Interventional Radiology, Hokkaido University Hospital, [3] Global Center for Biomedical Science and Engineering, Faculty of Medicine, Hokkaido University, [4] Department of Radiology, Faculty of Dental Medicine, Hokkaido University

Introduction: Exchange of water between the cerebrospinal fluid (CSF) and interstitial fluid (ISF) is considered a critical component of neurofluid dynamics. In recent years, increasing evidence has suggested that cerebral edema in the early phase of ischemia may be driven by the influx of water from the CSF into the brain parenchyma [1]. In this study, we investigated the CSF-ISF water exchange in a rat model of cardiac arrest by intrathecal administration of ^{17}O-labeled water ($H_2{}^{17}O$), visualized by proton MRI.

Materials & Methods: Ten male Wistar rats (8–10 weeks old) were used in this study. A cranial window was created using a drill to expose the dura mater, and a glass cannula was inserted into the subarachnoid space (SAS) [2]. A total of 28.4 μL of $H_2{}^{17}O$ (90% enrichment) was infused into the SAS at a rate of 1.8 μL/min. During the infusion, potassium chloride (KCl) was rapidly administered intravenously in the cardiac arrest group (n = 5), while saline was administered in the control group (n = 5). Dynamic T2-weighted images [3] were acquired (1 phase at 1 min 26 sec; 6 pre-contrast phases; 11 during-contrast phases; and 23 post-contrast phases). A rectangular region of interest (ROI) measuring approximately 1.2 × 1.2 mm was placed in the cerebral cortex directly beneath the injection site to measure signal intensity. The ^{17}O concentration was calculated for each phase [4]. Statistical analysis was performed using two-way ANOVA ($P < 0.05$).

Results: In the cardiac arrest group, ^{17}O concentration in the cerebral cortex directly beneath the injection site showed a slight increase during the $H_2{}^{17}O$ infusion (Fig.1 and 2). Following KCl-induced cardiac arrest, a sustained increase in ^{17}O concentration was observed after a brief delay. In contrast, in the control group, ^{17}O concentration also showed a slight increase during the infusion, similar to the cardiac arrest group, but gradually decreased after the infusion was stopped and returned to baseline levels.

Discussion: Using ^{17}O-labeled water MRI with intrathecal administration, we successfully visualized the exchange of water between CSF and ISF during global cerebral ischemia in a cardiac arrest rat model. A slight delay in the increase of ^{17}O concentration in the cerebral cortex was observed after the onset of ischemia, which may reflect CSF influx driven by a gradually developing osmotic gradient induced by ischemia.

Conclusions: The water movement in the hyperacute stage of cerebral ischemia was visualized by intrathecal administration of $H_2{}^{17}O$. Distribution of CSF-derived water into the brain parenchyma was confirmed during this early phase.

References:
[1] Science. 2020;367(6483):eaax7171. [2] Proc. Intl. Soc. Mag. Reson. Med. 33 (2025). [3] Magn Reson Med Sci. 2025;24(2):269-275. [4] Invest Radiol. 2024;59(1):92-103.

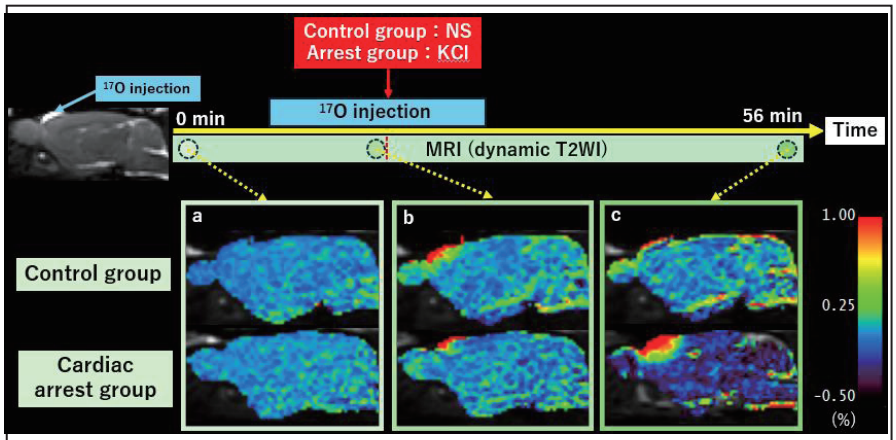

Fig. 1 Time-course changes in ^{17}O concentration maps following subarachnoid $H_2{}^{17}O$ injection in KCl- and normal saline (NS)- injected groups. (a) Before $H_2{}^{17}O$ injection, (b) During $H_2{}^{17}O$ injection and immediately before KCl or NS injection, (c) After KCl or NS injection

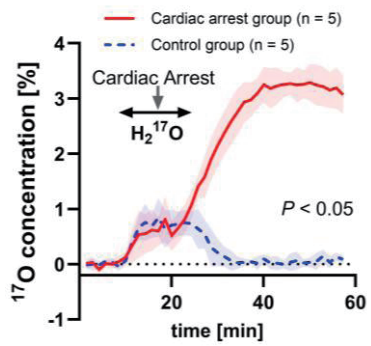

Fig. 2 Changes in ^{17}O concentration in the cortex after SAS injection of $H_2{}^{17}O$: KCl vs. saline groups. Bold lines show means: thin lines, SD. Arrows indicate $H2^{17}O$ injection and timing of KCl or sham treatment.

Oral Presentation 2

JPC-007

Comparison of 3D Diagonal and 3-Scan Trace Diffusion-Weighted Imaging for Breast MRI

Yusuke Jo[1,2], Mami Iima[2,3], Hiroko Satake[2], Yunhao Zhang[2], Yutaka Kato[2], Yuki Sato[2], Satoko Ishigaki[2], Ryota Hyodo[2,3], Yoshito Ichiba[4], and Shinji Naganawa[2]

1. Department of Radiology, Anjo Kosei Hospital, Aichi, Japan
2. Department of Radiology, Nagoya University Graduate School of Medicine, Nagoya, Japan
3. Department of Fundamental Development for Advanced Low Invasive Diagnostic Imaging, Nagoya University Graduate School of Medicine, Nagoya, Japan
4. Siemens Healthcare K.K., Tokyo, Japan

Introduction: Diffusion-weighted imaging (DWI) has become an integral component of breast MRI and is included in BI-RADS (1). Improving DWI quality might improve lesion detection. This study compared standard 3-scan trace DWI (tDWI) with 3D diagonal DWI (dDWI), offering faster acquisition and simplified gradients, using phantom and clinical assessment.

Materials & Methods: This prospective study (May–September 2024) included 92 patients with 69 breast lesions evaluated using 3.0T MRI. Both tDWI and dDWI were performed with identical TR (5000 ms) and TE (67 ms). Acquisition times were 120 s for tDWI and 74 s for dDWI. The gradient directions [x, y, z] were [1.0, 1.0, −0.5], [1.0, −0.5, 1.0], [−0.5, 1.0, 1.0] for tDWI and [1.0, 1.0, 1.0] for dDWI. Two observers rated lesion conspicuity and image quality on a 5-point scale (5: excellent- 1: not visible) (2). ADC values were measured, and agreement between tDWI and dDWI was assessed.

Results: dDWI showed equivalent or superior lesion conspicuity compared to tDWI (Observer 1: 3.62 ± 0.94 vs 3.84 ± 0.90 for tDWI and dDWI, p=0.02; Observer 2: 3.03 ± 0.70 vs 3.26 ± 0.81, p=0.08). Image quality scores were notably better for dDWI, (Observer 1: 3.07 ± 0.60 vs 3.49 ± 0.65, p<0.01; Observer 2: 3.25 ± 0.69 vs 3.45 ± 0.76, p<0.01). ADC values showed strong agreement between protocols (R^2: 0.98). Representative cases are shown in Figures 1 and 2.

Discussion & Conclusion: Despite reduced acquisition time (38%), dDWI maintained comparable quantitative accuracy with strong agreement in ADC measurements. dDWI demonstrated improved artifact management around challenging anatomical regions (Nipple areas and Chest wall). tDWI remains the standard approach, but dDWI might offer a valuable alternative in time-sensitive clinical scenarios.

References: 1. Iima M, et al. Diffusion MRI of the breast: Current status and future directions. J Magn Reson Imaging. 2020;52(1):70-90.
2. Kishimoto AO, et al. Evaluation of Malignant Breast Lesions Using High-resolution Readout-segmented Diffusion-weighted Echo-planar Imaging: Comparison with Pathology. Magn Reson Med Sci. 2021;20(2):204–215.

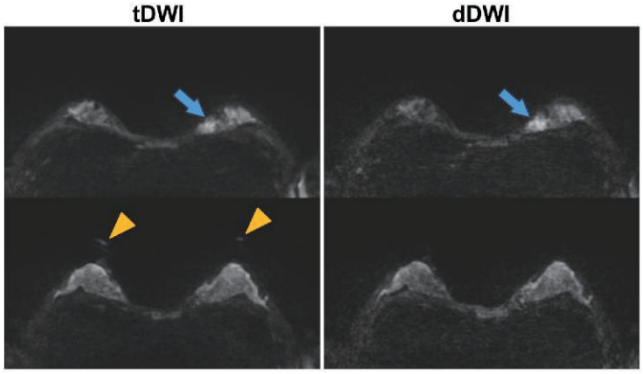

Fig.1 Comparison of lesion conspicuity and nipple artifacts between tDWI and dDWI (b = 800 s/mm²).
dDWI shows higher lesion conspicuity (blue arrows) and reduced magnetic susceptibility artifacts near nipples (yellow arrowheads) compared to tDWI, under identical display settings.

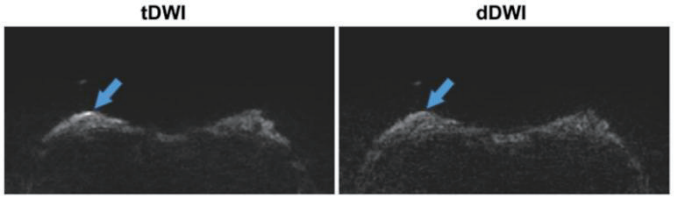

Fig2. Example of breast images obtained by tDWI and dDWI (b=800 s/mm²).
Artifacts observed along the breast tissue periphery (blue arrows) in tDWI are successfully eliminated in dDWI.

Oral Presentation 2

JPC-008

Automated Breast Cancer Detection and Classification Using Machine Learning on DWI

Kaito Nonoyama[1], Mami Iima[1, 4], Ryosuke Mizuno[2], Keiho Imanishi[3], Hiroko Satake[1], Rintaro Ito[1], Masako Kataoka[4], Shinji Naganawa[1]

[1]Department of Radiology, Nagoya University Graduate School of Medicine, Nagoya, Japan [2]A. I. System Research Co., Ltd., Kyoto, Japan, [3]e-Growth Co., Ltd., Kyoto, Japan, [2]Department of Radiology, Kyoto University Graduate School of Medicine, Kyoto, Japan

Introduction: Breast MRI shows high sensitivity for cancer detection but suboptimal specificity (1). While multi-b value DWI can improve diagnosis, it can increase workload (2). Thus, there is a strong need for automated diagnostic tools. Most AI research has focused on DCE MRI rather than DWI alone for lesion characterization (3). This study investigates AI for breast tumor detection and diagnosis in DWI.

Materials & Methods: This retrospective study evaluated 601 patients who underwent 3T MRI from May 2019 to March 2022. Among them, 392 patients with breast lesions were analyzed (41 test, 351 training/validation). Breast DWI was scanned using five b-values (0, 200, 800, 1000, 1500 s/mm²). All 48 slices per breast were independently input into a fine-tuned YOLO v5 to detect tumors, and a small 2D CNN (Fig.1) predicted the malignancy of the detected tumor from 1) the whole slice image containing it or 2) a cropped image based on the detected bounding box (Fig.2). Diagnostic performance was evaluated using ROC analysis.

Results: The study analyzed 82 breasts (32 malignant, 12 benign, and 38 normal fibroglandular tissue) from 41 patients using two methods. The whole slice method achieved AUC of 0.90, with sensitivity of 84.4%, specificity of 84.0%, and accuracy of 84.1%. The bounding box method resulted in AUC of 0.87, with higher sensitivity of 87.5% but lower specificity of 80.0% and accuracy of 82.9%.

Discussion & Conclusions: Our study has demonstrated that AI integration can significantly enhance DWI's diagnostic capabilities for breast cancer detection. The two methods showed different diagnostic profiles: the whole slice method achieved higher AUC (0.90 vs 0.87) and better specificity (84.0% vs 80.0%), potentially reducing false positives, while the bounding box method showed higher sensitivity (87.5% vs 84.4%). To the best of our knowledge, this is the first study to investigate breast lesions using AI without segmentation. This approach builds upon previous work demonstrating AI's efficacy in differentiating breast tumors using DWI without segmentation (4). Through enhanced DWI specificity, AI integration could significantly reduce false positives and unnecessary biopsies, lowering healthcare costs and minimizing patient anxiety. This study demonstrates high diagnostic performance of AI-assisted approaches in breast tumor detection and characterization using DWI. While the retrospective design and limited dataset size may affect generalizability, these findings support the clinical potential of the approach. Future work will focus on detection threshold optimization, evaluation with reduced b-value sets for clinical efficiency, and extension to BI-RADS score classification.

References: 1. Iima M, Honda M, et al. *J Magn Reson Imaging.* 2020;52(1):70-90., 2. Okazawa A, et al. *Magn Reson Med Sci.* 2024;23(4):438-448., 3. Lo Gullo R, Brunekreef J, et al. *J Magn Reson Imaging.* 2024;60(6):2290-2308., 4. Iima M, Mizuno R, et al. *Radiology: Artificial Intelligence.* 2024;7(1):e240206.

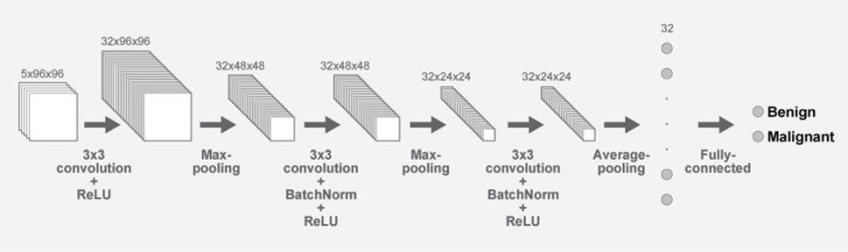

Fig.1: The architecture of small 2D CNN

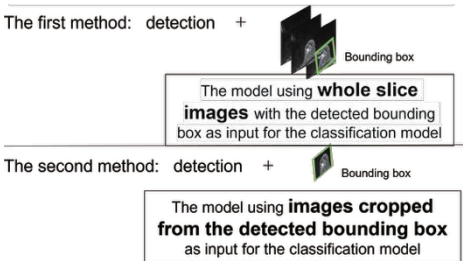

Fig.2: The processing step for deep leaning analysis

Oral Presentation 2

JPC-009

Usefulness of real-time sequence management in abdominal DWI MRI

Yuji Ohizumi[1], Shigeru Kiryu[1], Naoki Yoshioka[1], Masaaki Akahane[1], Kuni Ohtomo[2]

[1]Department of Radiology, International University of Health and Welfare Narita Hospital, 852 Hatakeda, Narita, Chiba, Japan, [2]Department of Radiology, International University of Health and Welfare, 2600-1 Kitakanemaru, Otawara, Tochigi, Japan.

Introduction: Diffusion-weighted imaging (DWI) plays a crucial role in diagnostic imaging these days. In particular, abdominal DWI has undergone advancements by incorporating various techniques. Among these, respiratory motion remains a significant challenge [1]. Eddy current is one of the factors that degrade the quality of MRI images, such as shading, blurring and geometric distortion. Recently, a new technology has been developed that enables real-time sequence control during MRI scanning due to high-speed communication systems, named Real-time Platform (Canon Medical Systems, Otawara, Japan). For eddy current compensation, conventional methods employ a fixed correction parameter derived from the repetition time (TR) variation prior to the scan. However, this approach causes a mismatch with the actual TR, which changes in response to the patient's respiratory state during the scan, resulting in degraded images. The Real-time Platform-applied DWI, proposed method, allows real-time adjustment of eddy current compensation according to the actual TR that changes with the patient's respiratory state. This technique is expected to improve image quality by optimizing eddy current compensation. In this study, we compared the conventional method and the proposed method, and assessed the effect of real-time sequence management in abdominal DWI MRI.

Materials & Methods: This prospective study was approved by our institutional review board, and written informed consent was obtained from the candidates. The upper abdominal DWI (b = 800 s/mm^2) was performed on 25 healthy volunteers in two sessions: before and after the introduction of Real-time Platform to a 3-T MRI scanner (Vantage Galan 3T, Canon Medical Systems, Otawara, Japan) with a 16-channel ventral body coil and a 32-channel dorsal spine coil. In qualitative analysis, two board-certified diagnostic radiologists independently evaluated all DWIs using six criteria scored on a 4-point Likert scale (4=good to 1=poor) on homogeneity and conspicuity of right and left hepatic lobes, overall noise, and overall image quality. In quantitative analysis, one operator reviewed all DWIs, and a circular region of interest (ROI) was placed on 3 points on the liver (cranial and caudal side of right hepatic lobe, and left hepatic lobe) and on the erector spinae muscles. For qualitative analysis, the scores were compared using the Wilcoxon signed-rank test. For quantitative analysis, the ratio of signal intensity of the ROI on the liver and the erector spinae muscles was compared using paired t-tests.

Results: Proposed method improved image quality in certain cases (Fig. 1), and in qualitative analysis, improved the left hepatic lobe depiction (homogeneity and conspicuity) and overall noise and image quality (Table 1). In quantitative analysis, there was no significant difference in the signal intensity of the liver between the conventional method and the proposed method.

Discussion: As expected, the proposed method tended to improve image quality. Improved image quality in the left hepatic lobe was observed with the proposed method. Since poor image quality in this region has been a well-known issue in DWI, this finding suggests that the proposed method makes a significant contribution to liver DWI. Although no statistically significant difference was found in the homogeneity of the right hepatic lobe, a trend toward improvement was observed with the proposed method (p = 0.074).

Conclusions: The new technology of real-time sequence control improved signal homogeneity and structure depiction in the left hepatic lobe, reduced overall noise, and enhanced image quality. Further studies involving a larger number of patients with hepatic lesions are needed.

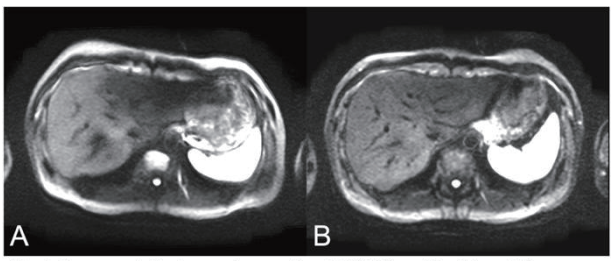

Fig. 1 A representable image of conventional DWI (A) and Real-time platform applied DWI (B).

Table 1 Results of qualitative analysis

		Convetional DWI	Proposed DWI	Comparison (p)
Right lobe	homogeneity	3.20 ± 0.775	3.40 ± 0.812	0.074
	conspicuity	3.24 ± 0.885	3.38 ± 0.875	0.111
Left lobe	homogeneity	2.28 ± 0.618	2.60 ± 0.721	0.007*
	conspicuity	2.10 ± 0.663	2.36 ± 0.700	0.016*
Overall noise		3.02 ± 0.640	3.32 ± 0.646	0.008*
Image quality		2.90 ± 0.529	3.14 ± 0.520	0.009*

Data are mean ± standard deviation of two observers' averaged scores

Comparisons were performed using Wilcoxon signed-ranks tests

DWI =Diffusion-weighted imaging

*A statistically significant difference (p < 0.05)

References:

1. Obara, Makoto et al. "Technical Advancements in Abdominal Diffusion-weighted Imaging." *Magnetic resonance in medical sciences : MRMS : an official journal of Japan Society of Magnetic Resonance in Medicine* vol. 22,2 (2023): 191-208. doi:10.2463/mrms.rev.2022-0107

Oral Presentation 2

JPC-010

Exploring Structural Brain Differences in OCD and SAD Using VBM and SBM

Nadire Aximu[1,2], Junbing He[2,3], Eiji Shimizu[1,2,3], Yoshiyuki Hirano[2,3]

[1]Department of Cognitive Behavioral Physiology, Graduate School of Medicine, Chiba University, Chiba, Japan, [2]Research Center for Child Mental Development, Chiba University, Chiba, Japan, [3]United Graduate School of Child Development, Osaka University, Suita, Japan

Introduction:

Social anxiety disorder (SAD) and obsessive-compulsive disorder (OCD) are distinct yet clinically overlapping conditions, both characterized by excessive anxiety and avoidance behaviors [1]. Although OCD is no longer classified as an anxiety disorder in DSM-5, it shares neural and symptomatic features with SAD. However, few studies have directly compared their brain structural differences. Voxel-Based Morphometry (VBM) and Source-Based Morphometry (SBM) are widely used techniques for analyzing structural Magnetic Resonance Imaging (MRI) data. VBM compares differences in gray and white matter volume, density, or concentration on a voxel-wise basis, while SBM identifies patterns of structural variation using independent component analysis. This study aims to compare the performance of VBM and SBM in detecting brain structural differences among individuals with OCD, SAD, and healthy controls (HC).

Materials & Methods:

The study included participants with OCD (n = 22), SAD (n = 24), and 28 HC, who matched in age, gender, and IQ. Differences in gray matter volume (GMV) and cortical complexity were compared using the one - way analysis of variance (ANOVA) and correlated with the clinical variables (LSAS, BDI-II, OCI-R and YBOCS) scores.

Results:

The VBM did not reveal any difference in GMV values in the three groups. Conversely, SBM analysis significantly decreased cortical thickness was found in the OCD group compared with HC in the right fusiform gyrus, right middle frontal gyrus, left superior frontal gyrus and right anterior cingulate cortex (Fig. 1).

Discussion:

Our research shows extensive cortical structural changes in the fusiform gyrus, middle frontal gyrus, superior frontal gyrus and anterior cingulate cortex regions in OCD. This provides a morphological perspective for understanding the pathophysiological mechanism underlying depression in Parkinson's disease.

Conclusions:

These findings demonstrate that SBM is a useful tool for revealing subtle brain structure differences in OCD.

References:

Storch E. A., Abramowitz J., Goodman W. K. (2008). Where does obsessive–compulsive disorder belong in DSM-V? Depress. Anxiety 25, 336–347. 10.1002/da.20488

Figures 1

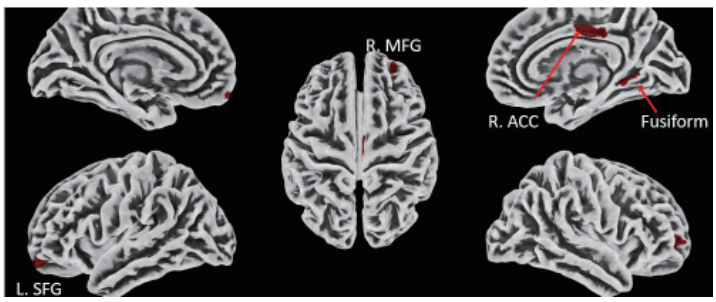

Oral Presentation 2

JPC-011

Cognitive traits and brain functions in older adults during the stroop task

Kazuya Ouchi[1,2], Tomokazu Tsurugizawa[1,2]

[1] National Institute of Advanced Industrial Science and Technology (AIST), [2] University of Tsukuba

Introduction:

Stroop task is one of the cognitive tests known to be related to executive function. Stroop task requires participants to respond to the color of a displayed color word, such as red and green. The response time is delayed when the color and meaning of the color word are incongruent (stroop effect). It is reported that older adults are more strongly affected by the stroop effect compared to younger (1). The response time during stroop task involves multiple cognitive components but the relationship between cognitive components and brain function has not been fully investigated. In this study, we used hierarchical drift diffusion model (HDDM) to estimate cognitive components, such as decision cautiousness and processing efficiency, and clarify how these components are associated with brain function.

Materials & Methods:

We conducted gradient echo echo planner imaging (TR / TE = 1,500 / 30 ms, isotropic voxel size = 2.5 mm, matrix size = 76 x 76, 44 slices, and 210 volumes.) during the stroop task in 27 older participants (68.6 ± 5.6 years). Decision cautiousness and processing efficiency were estimated using HDDM. Functional connectivity (FC) during stroop task was calculated from functional images, and its associations with the decision cautiousness and processing efficiency were examined. The functional connectivity during task was analyzed using generalized psychophysiological interaction approach (3).

Results:

As a result, decision cautiousness showed a significant negative correlation with FC between left Lateral sensorimotor area - right lateral prefrontal cortex (LPFC) ($r = -0.51$, $p < 0.01$) (Figure 1A), as well as between left Intraparietal Sulcus (IPS) - posterior cerebellar($r = -0.51$, $p < 0.01$) (Figure 1B). Additionally, left Intraparietal Sulcus - posterior cerebellar also exhibited a significant negative correlation with processing efficiency ($r = -0.50$, $p < 0.01$) (Figure 1C).

Discussion:

LPFC and IPS are core regions of the fronto-parietal netwok, which has been associated with executive function (2). In the present study, individuals with weak FC between the fronto-parietal network and sensorimotor or cerebellar regions tended to exhibit a more cautious and more efficient during stroop task. These findings contributes to a better understanding of age-related cognitive variability.

References:

(1) Ramos-Goicoa M et al. Effect of Normal Aging and of Mild Cognitive Impairment on Event-Related Potentials to a Stroop Color-Word Task. *J Alzheimers Dis*. 2016;52(4):1487-501.

(2) Hausman HK et al. Cingulo-opercular and frontoparietal control network connectivity and executive functioning in older adults. *Geroscience*. 2022;44(2):847-866.

(3) Tsurugizawa et al. Increased interhemispheric functional connectivity during non-dominant hand movement in right-handed subjects. iScience. 2023 ;26(9):107592.

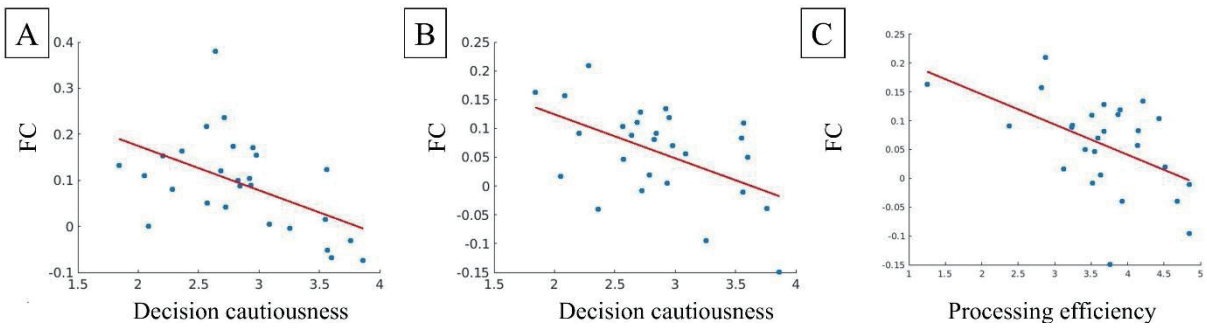

Fig 1 Correlations between HDDM parameters and functional connectivity (FC).

Oral Presentation 2

JPC-012

Hemostatic Radiotherapy for Gastric Cancer: MRI as an Alternative to Endoscopy for Post-Treatment Evaluation

Osamu Tanaka[1], Takuya Taniguchi[1], Shuto Nakaya[1], Kousei Adachi[1], Masayuki Matsuo[2]
[1]Department of Radiation Oncology, Asahi University, [2]Department of Radiology, Gifu University

Introduction: Pretreatment diagnosis by diffusion-weighted magnetic resonance imaging (DW-MRI) is useful to determine the effect of chemotherapy for gastric cancer. We previously reported the usefulness of the apparent diffusion coefficient (ADC) value after hemostatic radiotherapy (RT) for gastric cancer [1]. Here, we investigated the findings of relationship among DW-MRI, endoscopy, and tumor markers.

Materials & Methods: Eight patients underwent hemostatic RT for gastric cancer in this prospective study from 2019 to 2021. The patients completed MRI, endoscopy, and blood tests before RT; MRI, endoscopy, and blood tests 1 month after RT; and MRI and blood tests 3 months after RT. Correlations between changes in ADC derived from DW-MRI and the tumor marker carcinoembryonic antigen (CEA) were investigated.

Results: Univariate analysis of overall survival showed that sex and chemotherapy treatment were statistically significant factors. The CEA values before and 1 month after RT decreased significantly. There was no statistical difference between the CEA value 1 and 3 months after RT. The ADC value before and 1 month after RT increased significantly, but not between 1 and 3 months after RT. Comparing the ratio of ADC before RT to 1 (or 3) month(s) after RT with that of CEA before RT to 1 (or 3) month(s) after RT, we found an inverse relationship between the two ratios.

Discussion: The current study observed a correlation between changes in ADC and CEA. In addition, ADC may indicate a biological change earlier than CEA, and the ratios of ADC and CEA may be important factors for predicting the therapeutic effects of treatment.

Conclusions: Changes in ADC and CEA are correlated. Additionally, 3 months after RT, the decrease in ADC appeared earlier than the decrease in CEA. ADC may indicate a biological change earlier than CEA, and the ratios of ADC and CEA may be important factors. These aspects warrant further confirmation in a larger sample population.

References:
Tanaka O, Omatsu T, Kariya S, et al. Usefulness of diffusion-weighted magnetic resonance imaging for evaluating the effect of hemostatic radiotherapy for unresectable gastric cancer. Clin J Gastroenterol. 2019;12:269–73.

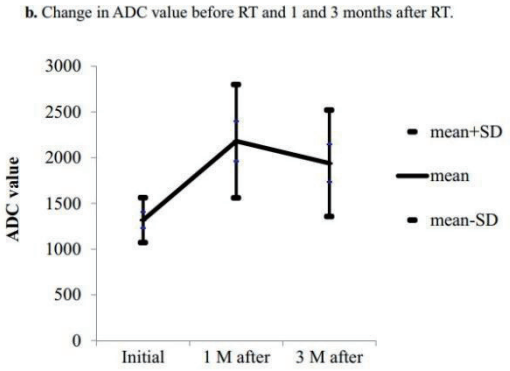

Figure legend

The ADC value before and1month after RT increased statistically significantly. *p<0.01.

There was no statistical difference between the ADC value 1

Oral Presentation 3

JPC-013

MR Elastography for Brain Tumors: Initial Experience

Tatsuya Oki[1], Neil Roberts[1,2], Maya Oki[1], Tomohiro Wataya[1], Akitoshi Inoue[1],
Ryuta Ito[1], Tadateru Fukami[3], Kazumichi Yoshida[3], Yoshiyuki Watanabe[1]
[1]Department of Radiology, Shiga University of Medical Science, [2]Clinical Research Imaging Centre, University of Edinburgh,
[3]Department of Neurosurgery, Shiga University of Medical Science

Introduction: MR Elastography (MRE) enables the noninvasive evaluation of brain tissue stiffness.[1] We report our initial experience with ten patients undergoing brain tumor MRE under Japan's Clinical Research Law.

Materials & Methods: We used a head-specific passive driver and acquired MRE images on a 3T MRI scanner with the following parameters: TR/TE, 4000/73.3 ms; FOV, 240 × 240 mm; matrix, 80 × 80; slice thickness, 3 mm; bandwidth, 250 kHz; motion-encoding gradient frequency, 60 Hz; external driver frequency, 60 Hz; driver amplitude, 20%; number of phase offsets/locations, 8; total acquisition time, 6 min 28 s.

A board-certified radiologist independently performed the following: (1) delineated the outer tumor margin using a freehand region of interest (ROI) on the magnitude image, (2) created an inner ROI by shrinking the outer ROI by approximately 2 mm, (3) transferred the inner ROI onto the stiffness map to calculate the shear stiffness (Figure 1).

Intraoperative tumor consistency was evaluated by a neurosurgeon using a 5-point scale (1 = softest, 5 = hardest).

Results: Patient demographics were as follows: 7 females and 3 males; mean age, 65 years. Diagnoses included pituitary adenoma (n = 5), meningioma (n = 2), vestibular schwannoma (n = 1), cholesterol granuloma (n = 1), and suspected demyelinating disease (n = 1).

The shear stiffness values on MRE and intraoperative tumor consistency scores are summarized in Table 1. No significant correlation was observed between MRE-derived shear stiffness and intraoperative consistency (r = 0.166).

Discussion: Shear stiffness values for meningiomas were higher than those for pituitary adenomas, which aligns with previous studies.[2] We plan to evaluate shear stiffness using fused preoperative MRI and MRE images. We also aim to explore Slip Interface Imaging (SII) to assess tumor adhesion and infiltration.[3]

Conclusions: We report our preliminary experience with brain tumor MRE. Further studies with larger cohorts are required to refine measurement protocols and establish standardized evaluation criteria.

Table 1. Shear stiffness values and intraoperative tumor consistency scores

Histological Diagnosis	Shear Stiffness [kPa]	Intraoperative tumor consistency
Pituitary Adenoma	1.429	2.00
Meningioma	2.130	3.75
Vestibular Schwannoma	2.977	4.00
Cholesterol Granuloma	2.190	1.00
Demyelinating Disease	1.956	3.00

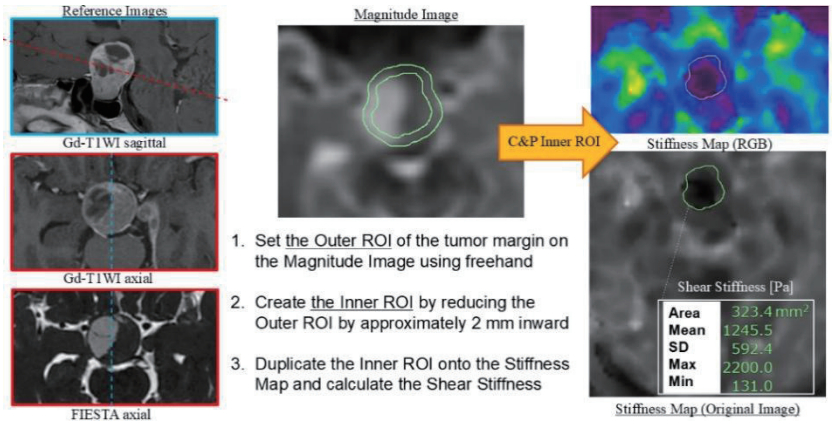

Figure 1. Measurement method of shear stiffness in MRE

References:

1. Bunevicius A, Schregel K, Sinkus R, Golby A, Patz S. REVIEW: MR elastography of brain tumors. Neuroimage Clin. 2020; 25:102109.

2. Sakai N, Takehara Y, Yamashita S, et al. Shear Stiffness of 4 Common Intracranial Tumors Measured Using MR Elastography: Comparison with Intraoperative Consistency Grading. AJNR Am J Neuroradiol. 2016; 37:1851-1859.

3. Yin Z, Glaser KJ, et al. Slip Interface Imaging Predicts Tumor-Brain Adhesion in Vestibular Schwannomas. Radiology. 2015; 277:507-517.

Oral Presentation 3

JPC-014

Clinical Feasibility: MR Elastography-based Slip Interface Imaging for Assessment of Myofascial Interface Mobility in Chronic Low Back Pain

Emi Hojo[1], Yi Sui[1], Xiang Shan[1], Keni Zheng[1], Phillip Rossman[1], Tim Waters[1], Armando Manduca[1], Garret M. Powell[1], Kai-Nan An[1], Richard L. Ehman[1], Sanjeev Nanda[1], Brent A. Bauer[1], and Ziying Yin[1]

[1]Mayo Clinic, Rochester, Minnesota

Introduction:

Myofascial dysfunction is considered to be a major contributor in chronic low back pain (CLBP) linked to myofascial pain syndrome (MPS) but lacks a quantitative imaging method[1]. Magnetic resonance elastography (MRE)-based slip interface imaging (SII)[2,3] quantifies inter-muscular mobility[4]. This study evaluated the clinical utility of the SII-derived maximal normalized displacement discontinuity (Dnorm)[5] to assess mobility at the quadratus lumborum-erector spinae (QL-ES) and erector spinae-multifidus (ES-M) interfaces at L3 and L4 in CLBP-MPS patients.

Materials & Methods:

20 CLBP-MPS patients (13 with comorbid fibromyalgia (FM)) and 20 age-, sex-, and BMI-matched healthy volunteers underwent 3T MRE with 30 Hz vibrations[6]. Patients were stratified by PEG (Pain, Enjoyment, and General Activity) scores into moderate-to-severe (PEG>4) and mild (PEG≤4) pain groups[7,8]. Dnorm-mobility index[4] was measured at L3 and L4 QL-ES and ES-M. Group differences were assessed using one-way ANOVA with Tukey's post-hoc test and Benjamini-Hochberg correction. Partial correlations between PEG and mobility were assessed, adjusting for FM and pain duration ($p<0.05$).

Results:

Significantly reduced mobility was found at the L4 ES-M interface in the moderate-to-severe group vs. controls ($p = 0.012$; $q = 0.026$) (Fig1). No other interface differences or significant PEG correlations were observed, though a moderate negative trend ($r = –0.40$) emerged at L4 ES-M.

Discussion & Conclusion:

Reduced mobility at the L4 ES-M interface in patients with more severe CLBP supports the role of biomechanical dysfunction in pain. However, the lack of strong correlation with PEG highlights the complex, multifactorial nature of CLBP, including central sensitization. SII-based Dnorm shows promise for identifying mechanical subtypes of CLBP, warranting further study in larger cohorts.

References:

1. Langevin HM. *Life (Basel)*. Jul 8 2021;11(7)doi:10.3390/life11070668
2. Yin Z, Glaser KJ, Manduca A, et al. *Radiology*. Nov 2015;277(2):507-17. doi:10.1148/radiol.2015151075
3. Yin Z, Hughes JD, Trzasko JD, et al. *J Magn Reson Imaging*. Oct 2017;46(4):1007-1016. doi:10.1002/jmri.25623
4. Hojo E, Sui Y, Shan X, et al. presented at: ISMRM 2025
5. Hojo E,Sui Y, Shan X, et al. presented at: ISMRM 2024
6. Yin Z, Sui Y, Trzasko JD, et al. *Magn Reson Med*. Dec 2018;80(6):2573-2585. doi:10.1002/mrm.27347
7. Krebs EE, Lorenz KA, Bair MJ, et al. *J Gen Intern Med*. Jun 2009;24(6):733-8. doi:10.1007/s11606-009-0981-1
8. Roldán-Majewski C, Broedel E, von Korff M, *PAIN*. 2022;163(4)

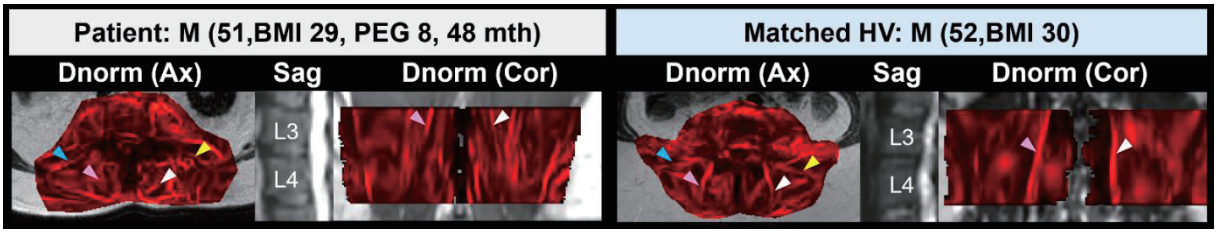

Fig1. Example Dnorm map comparison between a CLBP patient (Male, age 51, BMI 29, PEG 8, pain duration 48 months) and a matched healthy volunteer (Male, age 52, BMI 30). Axial (Ax) and coronal (Cor) views at L3–L4 are shown with sagittal (Sag) reference images. The patient shows low intensity at L4 ES-M interface on Dnorm. Arrows indicate QL-ES (blue: right, yellow: left) and ES-M (pink: right, white: left) interfaces. Dnorm maps are overlaid on T2-weighted (Ax) and MRE magnitude (Cor) images.

Oral Presentation 3

JPC-015

Evaluation of skeletal muscle energy metabolism before and after exercise using CEST MRI

Chisato Ando[1], Atsushi Takahashi[1], Takuya Ozawa[2], Kaito Takabayashi[2], Shuhei Shibukawa[1], Kou Yamanaka[3], Jimmy Kim[3], Nobuaki Mizuguchi[4], Kazuhiko Yamazaki[3], Takafumi Iwasaki[3], Ryutaro Yano[5], Seiko Shimizu[5], Hidefumi Waki[3], Eisuke Sato[1], Koji Kamagata[2], Shigeki Aoki[2], and Masaya Takahashi[1,2]

[1]Department of Radiological Technology, Graduate School of Health Science, Juntendo University, Tokyo, Japan, [2]Department of Radiology, Graduate School of Medicine, Juntendo University, Tokyo, Japan, [3]Department of Physiology, Graduate School of Health and Sports Science, Juntendo University, Chiba, Japan, [4]Juntendo Administration for Sports, Health and Medical Sciences, Juntendo University, Chiba, Japan, [5]Canon Medical Systems Corporation, Tokyo, Japan

Introduction: Adenosine triphosphate (ATP), the primary energy source for skeletal muscle contraction, is produced by three major ATP-generating pathways: 1) the ATP-creatine phosphate (PCr) system, 2) the anaerobic glycolysis, or lactic acid system, and 3) the aerobic system. The relative contribution of the ATP-generating pathway is determined by the type, intensity, and duration of exercise[1]. Chemical exchange saturation transfer (CEST) MRI enables the detection of the major ATP-generating substrates, excluding fatty acids[2]. Creatine (Cr), which is converted to phosphocreatine (PCr), is used in the pathway 1), and protein (Prot) and glucose (Glc) are used both in the pathways 2 and 3. We hypothesize that measures of the concentration changes of these substrates in the exercises may be able to estimate the ATP supply necessary in the local muscle. In this study, we first investigated whether CEST imaging is feasible to monitor the excise-related concentration changes of these substrates.

Materials & Methods: Twelve first-grade male athletes who belong to the track and field club at our college were subjected to this study. All subjects were positioned in the supine position (foot-first) in a 3-T MRI system (Vantage Galan, Canon Medical Systems) and performed a dorsiflexion exercise within the magnet, consisting of 50 seconds of dorsiflexion followed by 25 seconds of rest, repeated five times. CEST imaging was performed on an axial slice of the lower leg at 30% of the length from the proximal tibia, including both the tibialis anterior (TA), which is involved in dorsiflexion, and the soleus (So), which served as a control muscle. Imaging was conducted at four time points: before exercise (pre), and at 0 - 5 min (post1), 10 - 15 min (post2), and 20 - 25 min (post3) after exercise. The imaging parameters were: saturation pulse = 2 μT for 2 s, slice thickness = 5 mm, TR = 5000 ms, TE = 10 ms, FOV = 100 × 100 mm², matrix size = 128 × 128, and echo train length = 34. B0 correction was performed using the WASSR method. CEST images were acquired using a reference of 300 ppm, and saturation pulses applied every 0.25 ppm across the frequency range of -5 to +5 ppm. Voxel-wise z-spectra were obtained, and CEST signals were calculated from the MTR asymmetry analysis at the following frequency offsets: Cr at 2.0 ppm, Glc at 1.2 ppm, and Prot at 3.5 ppm. The statistical analysis was conducted by the Dunnett's multiple comparison test to compare signal changes at each time point with the pre-exercise baseline.

Results: Figure 1 shows the temporal changes in CEST signals for each substrate in TA and So. In the TA, the CEST signal for Cr increased immediately after exercise (post1, $p < .05$) and gradually returned to baseline levels over time. The Glc signal also increased immediately after exercise (post1, $p < .05$) , but decreased to lower than that in pre at post2 and post3 ($p < .01$). The Prot signal exhibited a similar trend; however, no statistically significant changes were observed.
In the So, no changes were observed in the Cr and Glc signals at post1; however, both significantly decreased at post2 compared to those at pre ($p < .05$). The Prot signal in the So remained unchanged throughout the protocol.

Discussion: In the TA, which is directly involved in the dorsiflexion exercise, increased Cr CEST signals are likely due to its conversion from PCr following ATP consumption[3]. The increased Glc signal may be explained by a combination of increased substrate delivery due to exercise-induced enhanced blood flow exceeding the rate of glucose consumption, and enhanced glucose uptake into muscle cells via insulin-independent mechanisms[4]. In contrast, the aerobic system responds more slowly, and under the short-duration exercise protocol used in this study, the change of the Prot signal might be subtle[1].

The decreased signals of Glc at post2 and 3 is considered the consumption of Glc for the anaerobic system 2) and the aerobic system 3) in order to resynthesize used ATP and glycogen. The cause of this decrease in the control So remains unclear, but one possible explanation is to influence the predominant supply of blood to the TA after excise. Further investigation of local blood flow is warranted to clarify this observation.

Conclusions: This study suggests that CEST imaging can detect changes in the tissue concentrations of multiple substrates involved in local energy metabolism necessary to exercise. In the future, establishing estimations of the relative contributions of each ATP-generating pathway might be a scientific tool to support nutritional strategies and supplementation tailored to the type and characteristics of the sport, as well as training and rehabilitation.

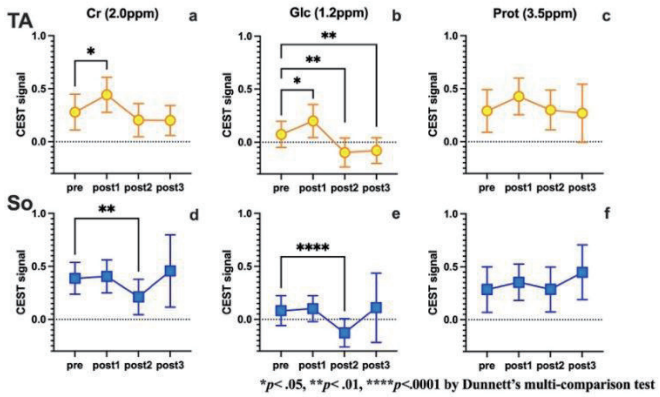

Fig 1. Time course of CEST signal changes for creatine (Cr: 2.0 ppm, a, d), glucose (Glc: 1.2 ppm, b, e), and protein (Prot: 3.5 ppm, c, f) in the tibialis anterior (TA) and soleus (So) muscles before and after dorsiflexion exercise.

References:

1. Hargreaves M, Spriet LS. Skeletal muscle energy metabolism during exercise. Nat Metab. 2020 Aug;2(8):817-828.
2. Kogan F, Hariharan H, et al. Chemical exchange saturation transfer (CEST) imaging: description of technique and potential clinical applications. Curr Radiol Rep. 2013 Feb 14;1(2):102-114.
3. Kogan F, Haris M, et al. In vivo CEST imaging of creatine (CrCEST) in skeletal muscle at 3T. J Magn Reson Imaging. 2013 Oct;40(3):596–602.
4. Rose AJ, Richter EA. Skeletal muscle glucose uptake during exercise: how is it regulated? Physiology (Bethesda). 2005 Aug;20:260-270.

Memo

SPONSORS　（協　賛）

AcroBio Corporation　（アクロバイオ株式会社）

AIRS Medical Japan　（エアーズメディカルジャパン合同会社）

BRACCO Japan　（ブラッコ・ジャパン株式会社）

BRUKER Japan　（ブルカージャパン株式会社）

Canon Medical Systems Corporation　（キャノンメディカルシステムズ株式会社）

Eli Lilly Japan K.K.　（日本イーライリリー株式会社）

FUJIFILM Medical Co., Ltd.　（富士フイルムメディカル株式会社）

GE HealthCare Japan　（GE ヘルスケア・ジャパン株式会社）

GE HealthCare Pharma　（GE ヘルスケアファーマ株式会社）

INFINITT JAPAN Co., Ltd.　（株式会社インフィニットジャパン）

J-MAC SYSTEM,INC.　（株式会社ジェイマックシステム）

Nemoto Kyorindo Co., Ltd.　（株式会社　根本杏林堂）

Philips Japan, Ltd.　（株式会社フィリップス・ジャパン）

PSP Corporation　（ピーエスピー株式会社）

UBIX Corporation　（ユビックス株式会社）

United Imaging Healthcare Japan K.K

（ユナイテッドイメージングヘルスケアジャパン株式会社）

（Sorted by Alphabetical ／　アルファベット順）

PHILIPS

Accelerating performance and precision

MR 7700

販　　売　　名：フィリップス Elition 3.0T

医療機器認証番号：230ACBZX00009000

設置管理医療機器／特定保守管理医療機器

管理医療機器

製造販売業者
株式会社フィリップス・ジャパン
www.philips.co.jp/healthcare

Innovation

Education

Sustainability

Trust

BRACCO

LIFE FROM INSIDE

ブラッコ・ジャパン株式会社
〒171-0022 東京都豊島区南池袋1-13-21
www.bracco.com/ja

文献請求先及び問い合わせ先：ブラッコ・ジャパン株式会社
フリーダイヤル 0120-318-170
（受付時間9～17時　土･日･祝日、会社休日を除く）

BJ-20250205-02


ISMRM
Japanese Chapter